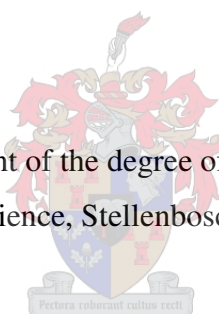


Preparation and Coordination Chemistry of Bis-Pyridyl Diamide Ligands

by
Eustina Batisai

Thesis presented in partial fulfilment of the degree of Master of Science in Chemistry at
Faculty of Science, Stellenbosch University



Supervisor
Professor L. J. Barbour

Co-supervisor
Dr. T. le Roex

March 2010

Declaration

By submitting this dissertation electronically, I declare that the entirety of the work contained therein is my own, original work, that I am the owner of the copyright thereof (unless to the extent explicitly otherwise stated) and that I have not previously in its entirety or in part submitted it for obtaining any qualification.

Eustina Batisai

March 2010

Copyright © 2010 Stellenbosch University

All rights reserved

Abstract

The number of coordination complexes utilizing bis-pyridyl diamide ligands has increased significantly over the past decade. This is attributed to the relatively easy synthetic procedure of the ligands and interesting structural features such as helicity, water clusters and porosity that the coordination complexes possess. In the first part of this study, the following eight structurally related bis-pyridyl diamide ligands:

- *N,N'*-bis(pyridin-4-ylmethyl)isophthalamide (**ISO**);
- *N,N'*-bis(pyridin-4-ylmethyl)terephthalamide (**TER**);
- *N,N'*-bis(pyridin-4-ylmethyl)hexanediamide (**ADI**);
- *N,N'*-bis(pyridin-4-ylmethyl)butanediamide (**SUC**);
- *N,N'*-bis(pyridin-4-ylmethyl)biphenyl-4,4'-dicarbonyl dicarboxamide (**DIP**);
- *N,N'*-dipyridin-2-ylpentanediamide (**GLUT**);
- (*2E*)-*N,N'*-bis(2-pyridin-4-ylmethyl)but-2-enediamide (**FUM**);
- 4-(pyridin-4-ylmethyl)aminocarbonyl benzoic acid (**TER-A**).

were synthesized and characterized by NMR, FTIR, MS and SCD. In the second part, the synthesized ligands were reacted with a variety of transition metal salts to yield fifteen novel coordination polymers and one discrete complex. SCD analysis showed that of the sixteen complexes thirteen formed 1-D chains, two formed 2-D networks, and one formed a discrete unit. Hydrogen bonding interactions between water molecules, the counterions and the amide groups resulted in connection of the lower dimension entities into higher dimension networks. The synthesized ligands were co-crystallized with trimesic acid and a novel co-crystal consisting of **ADI** and trimesic acid was obtained. SCD analysis showed that the co-crystal featured the amide homosynthon as well as the pyridine/carboxylic acid heterosynthon.

Opsomming

Die aantal koördinasie komplekse met dipiridiediamied ligande het noemenswaardig vermeerder oor die afgelope dekade. Hierdie groei kan toegeskryf word aan die eenvoudige sintetiese prosedure en interessante strukturele eienskappe van dié koördinasie komplekse, wat o.a. helikse, waterbondels en poreuse materiale vorm. In die eerste deel van hierdie studie is die agt onderstaande struktureel verwante dipiridiediamied ligande se sintese en karakterisering deur kernmagnetieseresonansie, Fourier transform infrarooi, massaspektrometrie en enkel kristal X-straal diffraksie (SCD) beskryf:

- *N,N'*-bis(piridien-4-ielmetiel)isoftalamied (**ISO**);
- *N,N'*-bis(piridien-4-ielmetiel)tereftalamied (**TER**);
- *N,N'*-bis(piridien-4-ielmetiel)heksaandiamied (**ADI**);
- *N,N'*-bis(piridien-4-ielmetiel)butaandiamied (**SUC**);
- *N,N'*-bis(piridien-4-ielmetiel)bifeniel-4,4'-dikarboniëdikarboksamied (**DIP**);
- *N,N'*-dipiridien-2-ielpentaandiamied (**GLUT**);
- (2E)-*N,N'*-bis(2-piridien-4-ielmetiel)but-2-eendiamied (**FUM**);
- 4-(piridien-4-ielmetiel)aminokarbonië bensoësuur (**TER-A**).

In die tweede gedeelte is bg. ligande met 'n reeks oorgangsmetaalsoute gereageer om vyftien nuwe koördinasiepolimere, asook een diskrete kompleks, te lewer. SCD analise toon dat van hierdie sestien komplekse vorm dertien 1-D kettings, twee vorm 2-D netwerke en slegs een vorm 'n diskrete eenheid. Waterstofbindings tussen die water molekules, die teen-ione en die amied groepe het laer dimensie (1-D) eenhede verbind om hoër dimensionele netwerke (2-D) te vorm. Mede-kristallisatie van die gesintetiseerde ligande met trimesiesuur het 'n nuwe mede-kristal tussen ADI en triemesiesuur opgelewer. Enkelkristal diffraksie toon dat die mede-kristal beide die amied homosinton en die piridien/karboksiësuur heterosinton bevat.

Acknowledgements

I would like to thank my supervisors, Professor Len Barbour and Dr Tanya le Roex for their guidance, financial and academic support throughout the course of this study and during the preparation of this manuscript. I would also like to extend my sincere gratitude to the following;

- Dr Jan-André Gertenbach for his help with SCD analysis;
- Dr Dinabandhu Das for his help with the synthetic part of this study;
- The Supramolecular Materials Chemistry Group members, past and present, at the University of Stellenbosch: Prof. Len Barbour, Dr Tanya Le Roex, Marlene Milani, Dr Martin Bredenkamp, Dr Catharine Esterhuysen, Dr Jan-André Gertenbach, Dr Delia Haynes, Dr Dinabandhu Das, Dr Subhadip Neogi, Dr Tia Jacobs, Charl Marais, Storm Potts, Leigh Loots, Bettinah Chipimpi, Dr Matteo Lusi, Anneli Kleyn, Dr Vincent Smith, Guillaume Greylin, Ilne Grobler, Charl Bezuidenhout, Helene Wahl, Marika Du Plessis and Dr Prashant Bhatt;
- The National Research Foundation (NRF) for funding;
- My family and friends for support and encouragement;
- James for proofreading some parts of this manuscript and for being the best partner I could ever ask for.

Above all I would like to thank the Lord Almighty for the gift of life.

To my parents, Mainini Mai Ngoni, my siblings, my little girl and my dearest husband.

Table of Contents

Declaration	i
Abstract	ii
Opsomming	iii
Acknowledgements	iv
Table of Contents	vi
List of Schemes	xv
Atomic Colour Scheme	xviii
Glossary of Terms	xix
Chapter 1. Crystal Engineering	1
1.0. Introduction	1
1.1 Tectons and supramolecular synthons	2
1.2 Intermolecular interactions	4
1.2.1 Directional forces.....	4
1.2.2 Non-directional forces	6
1.3 Self assembly	6
1.4 Coordination polymers	8
1.4.1 Coordination complexes of ligands containing the bis-pyridyl and amide functionalities	10
1.4.2 Properties of coordination complexes of bis-pyridyl diamide ligands	11
1.5 Aims and objectives.....	16
1.6 References.....	18
Chapter 2. Experimental	21
2.1 Synthesis and characterization of ligands	21
2.1.1 Preparation of <i>N,N'</i> -bis(pyridin-4-ylmethyl)isophthalamide (ISO)	21
2.1.2 Preparation of <i>N,N'</i> -bis(pyridin-4-ylmethyl)terephthalamide (TER)	22
2.1.3 Preparation of (2E)- <i>N,N'</i> -bis(2-pyridin-4-ylethyl)but-2-enediamide (FUM)	22
2.1.4 Preparation of <i>N,N'</i> -bis(pyridin-4-ylmethyl)succinamide SUC.....	23
2.1.5 Preparation of <i>N,N'</i> -bis(pyridin-4-ylmethyl)hexanediamide (ADI)	23
2.1.6 Preparation of <i>N,N'</i> -bis(pyridin-4-ylmethyl)biphenyl-4,4'-dicarbonyl dicarboxamide (DIP)	24
2.1.8 Preparation of <i>N,N'</i> -dipyridin-2-ylpentanediamide (GLUT)	24
2.1.9 Preparation of 4-(pyridin-4-ylmethyl)aminocarbonyl benzoic acid (TER-A).....	25

2.2	Crystallizations of the ligands with metal salts.....	25
2.2.1	Solvent evaporation method	25
2.2.2	Solvothermal method	26
2.2.3	Layering method	26
2.3	Instrumentation and computer packages.....	35
2.3.1	Single Crystal Diffraction Analysis (SCD).....	35
2.3.2	X-ray Powder Diffraction (PXRD).....	36
2.3.3	Nuclear Magnetic Resonance (NMR).....	36
2.3.4	FTIR-ATR.....	36
2.3.5	Liquid Chromatography Electrospray Ionisation Mass Spectrometry	36
2.3.6	The Cambridge Structural Database (CSD).....	36
2.4	References.....	36
Chapter 3. Crystal Structure Descriptions of the Pure Ligands		38
3.1	Introduction.....	38
3.2	Crystal structure descriptions of the pure ligands.....	38
3.2.1	Crystal structure of TER, the tetrahydrate	38
3.2.2	Crystal structure of TER, the dihydrate	40
3.2.3	Crystal structure of ADI.....	42
3.2.4	Crystal structure of DIP	43
3.2.5	Crystal structure of GLUT	45
3.2.6	Crystal structure of TER-A	46
3.3	Conclusion	47
3.4	References.....	48
Chapter 4. Coordination Chemistry of Bis-Pyridyl Diamide Ligands.....		50
4.1	Introduction.....	50
4.2	Results and discussion: Crystal structure determinations from SCD analysis.	50
4.2.1	Crystal structures obtained with FUM.....	50
4.2.2	Crystal structures obtained with SUC.....	61
4.2.3	Comparison of complexes 1-5	62
4.2.4	Crystal structures obtained with ADI	63
4.2.6	Crystal structures obtained with GLUT	82
4.2.6	Crystal structures obtained with ISO	87
4.2.7	Crystal structures obtained with TER-A.....	89
4.4	References.....	93
Chapter 5. Conclusion		98

5.1	Concluding remarks	98
5.2	References.....	99
	Appendices.....	100

List of Figures

Figure 1.1. Comparison between molecular synthesis and supramolecular synthesis.	1
Figure 1.2. (a) The definition of the geometric parameters for a hydrogen bond, (b) bifurcated and (c) trifurcated hydrogen bond.	5
Figure 1.3. Three types of interactions possible between the phenyl rings.	6
Figure 1.4. Generation of a 2-D network <i>via</i> self assembly of 4-(pyridin-4-ylmethyl)aminocarbonyl benzoic acid (TER-A). The individual molecules interact <i>via</i> the pyridine/carboxylic acid heterosynthon and the amide homosynthon.	7
Figure 1.5. Three types of networks that can be constructed using polydentate ligands and metal ions.	9
Figure 1.6. (a) The (H ₂ O) ₁₀ water cluster in 1 and (b) comparison between the water cluster (red) and ice Ic (blue). The three unique water molecules are labelled a, b and c.	12
Figure 1.7. (a) The M ₆ (BEN) ₈ cage, (b) the M ₆ (BEN) ₈ cage as well as the outer and inner water clusters.	13
Figure 1.8. Schematic diagram the M ₆ (BEN) ₈ cage. The pale yellow octahedron represents the M ₆ (BEN) ₈ cage. The inner and outer clusters are shown in blue and red, respectively	13
Figure 1.9. Schematic diagram showing single (black) and triple (red, blue and green) helices in {[Cd(succinate)(SUC-1)]·H ₂ O} _n . The metal centres are shown as black circles.	14
Figure 1.10. The double helix as well as the space filling model of Cu(SUC-2) ₂ ·(H ₂ O) ₂ . The strands of the double helix are coloured in green and red to distinguish them from one another.	14
Figure 3.1. The molecular structure of TER showing the crystallographic labelling scheme for the asymmetric unit and 50% probability ellipsoids for non hydrogen atoms. Red dashed lines indicate hydrogen bonding. The three planes are labelled a, b and c.	38
Figure 3.2. The packing diagram of TER-1 as viewed down the a axis. The region with the ellipse is shown magnified in Figure 3.3.	39

Figure 3.3. An expanded view of the hydrogen bond interaction between individual TER and water molecules.....	40
Figure 3.4. The molecular structure of TER-2 showing ellipsoids at 50% probability level and crystallographic labelling scheme. Only the asymmetric unit is labelled.	40
Figure 3.5. The packing diagram of TER-2. Individual TER molecules interact <i>via</i> the water molecule.	41
Figure 3.6. The 2-D networks formed as a result of the hydrogen bonding interactions between the water and TER molecules. The individual 2-D sheets are coloured in light brown and CPK colours to distinguish them from each other.	41
Figure 3.7. The molecular structure of ADI showing crystallographic labelling scheme and 30% probability ellipsoids for non-hydrogen atoms. Asymmetric unit atoms are labelled. Red dashed lines indicate hydrogen bonding.	42
Figure 3.8. ADI molecules pack in the herringbone motif; molecules in the same column interact <i>via</i> self-complementary amide hydrogen bonds and molecules in adjacent columns are linked by hydrogen bonding <i>via</i> water molecules. Hydrogen atoms not involved in hydrogen bonding have been omitted for clarity.	43
Figure 3.9. The molecular structure of DIP showing ellipsoids at 50% probability level and the crystallographic labelling scheme for the asymmetric unit. Red dashed lines indicate hydrogen bonding.	43
Figure 3.10. The packing diagram of DIP as viewed along the a axis. The region with the inserted circle is shown magnified in Figure 3.11.	44
Figure 3.11. The expanded view of the hydrogen bonding interaction between DIP and water molecules.	45
Figure 3.12. The asymmetric unit of GLUT showing the crystallographic labelling scheme and displacement ellipsoids at 50% probability level.	45
Figure 3.13. (a) Crisscross 1-D chains formed as a result of hydrogen bond interaction between amide NH and aromatic CH groups of neighbouring GLUT molecules, (b) packing diagram showing chains in the two layers coloured in light brown and CPK colours.	46
Figure 3.14. The asymmetric unit of TER-A showing the crystallographic labelling scheme and 50% probability ellipsoids for non hydrogen atoms.	47

Figure 3.15. The packing diagram of TER-A. Individual TER-A molecules interact <i>via</i> complementary amide to amide hydrogen bonds as well as PY-N \cdots H-O hydrogen bonds.....	47
Figure 4.1. The molecular structure of 1 showing crystallographic labelling scheme and 50% probability ellipsoids for non-hydrogen atoms. Only the asymmetric unit is labelled.	50
Figure 4.2. 2-D hydrogen bonded network formed as a result of interactions between the amide groups, the sulphate anions and coordinated water molecules. Only the atoms involved in hydrogen bonding are labelled.	51
Figure 4.3. Packing diagram of 1. Chains in alternate layers are shown in red and blue to distinguish them from one another, the sulphate anions are shown in CPK colours. The water molecules and hydrogen atoms have been omitted for clarity.	52
Figure 4.4. Expanded view of the hydrogen bonding interactions between layers, sulphate anions link the chains in alternate layers <i>via</i> hydrogen bonding to coordinated water molecules.....	53
Figure 4.5. The molecular structure of 2 showing crystallographic labelling scheme and 50% probability ellipsoids for non-hydrogen atoms. Only the asymmetric unit is labelled.	53
Figure 4.6. The packing diagram of as viewed along [001]. Chains in the adjacent layers are shown in CPK colours and in light brown.	54
Figure 4.7. Hydrogen bonding interactions between chains in the same layer. The 1-D chains interact <i>via</i> the nitrate anion. Only the atoms involved in hydrogen bonding have been labelled.....	55
Figure 4.8. Hydrogen bonding interactions between chains in adjacent layers. The chains are shown in light brown and in CPK colours. Only the atoms involved in hydrogen bonding have been labelled.....	56
Figure 4.9. The molecular structure of 3 showing the crystallographic labelling scheme and 50% probability ellipsoids for non hydrogen atoms. Red dashed lines indicate hydrogen bonding, only the asymmetric unit is labelled.	57
Figure 4.10. The packing diagram of 3 as viewed along [001].	58
Figure 4.11. The 2-D chain interact <i>via</i> chloride anions to form a 2-D network in the <i>ab</i> plane.....	58

Figure 4.12. An expansion of the hydrogen bonding interactions between adjacent layers. The chains in adjacent layers have been coloured in blue and maroon to distinguish them from one another.	59
Figure 4.13. The molecular structure of 4 showing crystallographic labelling scheme and 50% probability ellipsoids for non hydrogen atoms. Red dashed lines indicate hydrogen bonding.....	60
Figure 4.14. The molecular structure of 5 showing crystallographic labelling scheme and 50% probability ellipsoids for non hydrogen atoms. Only the asymmetric unit is labelled.....	61
Figure 4.15. The asymmetric unit of 6 showing 50% probability ellipsoids for non-hydrogen atoms. Only the asymmetric unit is labelled.....	64
Figure 4.16. Coordination geometric parameters around the Cd(II) centre.	64
Figure 4.17. 2-D network formed as a coordination bonds between the Cd(II) centre and the three independent ligands.....	65
Figure 4.18. Capped stick representation of 2-D nets . The nets interact <i>via</i> a coordination bond between the amide carbonyl group as well as a self-complementary amide bond. The other two nets have been omitted for clarity.....	66
Figure 4.19. The packing diagram of 6 showing all four 2-D nets. The nets have been coloured in different colours to distinguish them from one another. The hydrogen bonding and the coordination bonds have been omitted for clarity.	66
Figure 4.20. The molecular structure of 7 showing crystallographic labelling scheme and 50% probability ellipsoids for non hydrogen atoms. Only the asymmetric unit is labelled.	67
Figure 4.21. The packing diagram of 7 viewed along [010].	68
Figure 4.22. 2-D network formed as a result of hydrogen bonding interactions between S shaped units as viewed along [-101].....	69
Figure 4.23. The molecular structure of 8 showing crystallographic labelling scheme and 50% probability ellipsoids for non-hydrogen atoms. Only the asymmetric unit is labelled.....	70
Figure 4.24. The molecular structure of 9 showing the crystallographic labelling scheme and 50% probability for non-hydrogen atoms. Only the asymmetric unit is labelled.....	70

Figure 4.25. The molecular structure of 10 showing the crystallographic labelling scheme and 50% probability for non-hydrogen atoms. Only the asymmetric unit is labelled.	71
Figure 4.26. Capped stick representation of the hydrogen bond interaction between 1-D chains. The 1-D chains are linked <i>via</i> the nitrate anion and the water molecule into a 2-D network.	72
Figure 4.27. The packing diagram of complexes 8, 9 as 10 viewed along [010]. The hydrogen atoms have been omitted for clarity.	74
Figure 4.28. The asymmetric unit of 11 showing the crystallographic labelling scheme and 50% probability ellipsoids for non-hydrogen atoms. Only the asymmetric unit is labelled.	74
Figure 4.29. The packing diagram of 11 viewed along [010]. The hydrogen atoms have been omitted for clarity.	75
Figure 4.30. An expansion of the hydrogen bonding interactions between the 1-D chains.	76
Figure 4.31. The molecular structure of 11 showing the crystallographic labelling scheme and 50% probability ellipsoids for non hydrogen atoms. Only the asymmetric unit is labelled.	77
Figure 4.32. The molecular structure of ADI and trimesic acid co-crystal showing the crystallographic labelling scheme and 50% probability ellipsoids for non-hydrogen atoms.	78
Figure 4.33. A 2-D sheet formed as a result of hydrogen bond interaction and weak between Trimesic acid and ADI.	79
Figure 4.34. The packing diagram of the ADI and trimesic acid co-crystal viewed along [100]. The trimesic acid molecules have been coloured in light brown and the ADI molecules are shown in CPK colours. Hydrogen atoms not involved in hydrogen bonding have been omitted for clarity.	79
Figure 4.35. The molecular structure of 14 showing crystallographic labelling scheme and 50% probability ellipsoids for non-hydrogen atoms. Only the asymmetric unit is labelled.	83
Figure 4.36. Spiral 1-D chains viewed along [100].	83
Figure 4.37. The 1-D chains interact <i>via</i> the nitrate anions to form a 2-D layer.	84
Figure 4.38. The packing diagram of 14. The chains in the two distinct layers have been coloured in light brown and CPK colours to distinguish them from one another. The hydrogen atoms have been omitted for clarity.	85

Figure 4.39. The molecular structure of 15 showing atomic labelling scheme and 50% probability ellipsoids for non hydrogen atoms. Only the asymmetric unit is labelled.	86
Figure 4.40. The asymmetric unit of 16 showing crystallographic labelling scheme and 50% probability ellipsoids for non-hydrogen atoms.....	87
Figure 4.41. (a) 1-D lopped chains, (b) the packing diagram as viewed along [100]	88
Figure 4.42. An expanded view of the hydrogen bond interactions occurring between 1-D chains.	89
Figure 4.43. The asymmetric unit of 17 showing probability ellipsoids at 30% level and atomic labelling scheme.....	90
Figure 4.44. The metal centres are linked by ligand molecules to form a 2-D network which has channels along the a axis. The water molecules, DMF molecule and the hydrogen atoms have been omitted for clarity.....	90
Figure 4.45. The packing diagram of 17 viewed along [100]. The ligand molecules are shown in capped stick format while the DMF is shown with van der Waals radii.	91

List of Schemes

Scheme 1.1. Some common supramolecular synthons.....	3
Scheme 1.2. (a) The bipyridine ligand and bis-pyridyl based ligands containing (b) the urea or (c) oxalamide functionality.....	10
Scheme 1.3. The general structure of bis-pyridiyl diamide ligands and the various spacers	11
Scheme 1.4. (a) ISO, the first ligand consisting of an amide functionality and pyridine moiety to be presented in literature, (b) Tritopic ligand BEN	12
Scheme 1.5. Isomeric ligands (a) SUC-1 and (b) SUC-2.....	13
Scheme 1.6. Eight structurally related ditopic ligands synthesized for this study.	18
Scheme 2.1. Synthesis of <i>N,N'</i> -bis(pyridin-4-ylmethyl)isophthalamide.	21
Scheme 2.2. Synthesis of <i>N,N'</i> -bis(pyridin-4-ylmethyl)terephthalamide.....	22
Scheme 2.3. Synthesis of (2 <i>E</i>)- <i>N,N'</i> -bis(2-pyridin-4-ylethyl)but-2-enediamide.....	22
Scheme 2.4. Synthesis of <i>N,N'</i> -bis(pyridin-4-ylmethyl)hexanediamide.....	23
Scheme 2.5. Synthesis of <i>N,N'</i> -bis(pyridin-4-ylmethyl)biphenyl-4,4'-dicarbonyl dicarboxamide.....	24
Scheme 2.6. Synthesis of <i>N,N'</i> -dipyridin-2-ylpentanediamide.....	24
Scheme 2.7. Synthesis of 4-(pyridin-4-ylmethyl)aminocarbonyl benzoic acid.....	25

List of Tables

Table 1.1	Characteristics of very strong, strong and weak hydrogen bonds.	5
Table 1.2	Comparison of the three complexes 3-5.....	16
Table 2.1.	Explanation of symbols used in Tables 2.2-2.10 to describe types of products obtained.....	26
Table 2.2.	Crystallizations of FUM with a variety of metal salts.....	27
Table 2.3.	Crystallizations of SUC with a variety of metal salts.....	28
Table 2.4.	Crystallizations of ADI with a variety of metal salts	29
Table 2.5.	Crystallizations of GLUT with a variety of metal salts.....	30
Table 2.6.	Crystallizations of ISO with a variety of metal salts.....	31
Table 2.7.	Crystallizations of TER with a variety of metal salts.....	32
Table 2.8.	Crystallizations of TER-A with a variety of metal salts.....	33
Table 2.9.	Crystallizations of DIP with a variety of metal salts.....	34
Table 2.10.	Co-crystallizations of trimesic acid (T) with the synthesized ligands (L).....	35
Table 3.1.	Hydrogen-bond geometry (\AA , $^\circ$) for TER-1	39
Table 3.2.	Hydrogen-bond geometry (\AA , $^\circ$) for TER-2	41
Table 3.3.	Hydrogen-bond geometry (\AA , $^\circ$) for ADI.....	42
Table 3.4.	Hydrogen-bond geometry (\AA , $^\circ$) for DIP.....	45
Table 3.5.	Hydrogen-bond geometry (\AA , $^\circ$) for TER-A.	47
Table 3.6.	Crystallographic data of the synthesized ligands	49
Table 4. 1.	Coordination geometry (\AA , $^\circ$) for 1	51
Table 4.2.	Hydrogen-bond geometry (\AA , $^\circ$) for 1.	52
Table 4.3.	Coordination geometric parameters (\AA , $^\circ$) for 2.	55
Table 4.4.	Hydrogen-bond geometry (\AA , $^\circ$) for 2.	56
Table 4.5.	Coordination geometric parameters (\AA , $^\circ$) for 3.	57
Table 4.6.	Hydrogen-bond geometry (\AA , $^\circ$) for 3.	59
Table 4.7.	Coordination geometric parameters (\AA , $^\circ$) for 4.	60
Table 4.8.	Hydrogen-bond geometry (\AA , $^\circ$) for 4.	60
Table 4.9.	Coordination geometric parameters for (\AA , $^\circ$) 5.	61

Table 4.10. Hydrogen-bond geometry (Å, °) for 5.	62
Table 4.11. Comparison of complexes 1-5.....	63
Table 4.12. Coordination geometric parameters (Å, °) for 6.....	63
Table 4.13. Hydrogen-bond geometry (Å, °) for 6.	65
Table 4.14. Coordination geometric parameters (Å, °) for 7.....	68
Table 4.15. Hydrogen-bond geometry (Å, °) for 7.	69
Table 4.16. Coordination geometric parameters (Å, °) for 8.	71
Table 4.17. Hydrogen-bond geometry (Å, °) for 8.	72
Table 4.18. Coordination parameters (Å, °) for 9.....	72
Table 4.19. Hydrogen-bond geometry (Å, °) for 9.	73
Table 4.20. Coordination geometric parameters (Å, °) for 10.....	73
Table 4.21. Hydrogen-bond geometry (Å, °) for 10.	73
Table 4.22. Coordination geometric parameters (Å, °) for 11.....	76
Table 4.23. Hydrogen-bond geometry (Å, °) for 11.	76
Table 4.24. Coordination geometric parameters (Å, °) for 12.....	77
Table 4.25. Hydrogen-bond geometry (Å, °) for 13.	79
Table 4.26. Conformations of ADI.....	80
Table 4.27. Comparison of crystal structures obtained with AD1.	82
Table 4.28. Coordination geometric parameters (Å, °) for 14.....	84
Table 4.29. Hydrogen-bond geometry (Å, °) for 14.....	84
Table 4.30. Coordination geometric parameters (Å, °) for 15.....	86
Table 4.31. Hydrogen-bond geometry (Å, °) for 15.....	86
Table 4.32. Coordination bond geometry (Å, °) for 16.....	88
Table 4.33. Hydrogen-bond geometry (Å, °) for 16.....	89
Table 4.34. Coordination geometric parameters (Å, °) for 17.....	91

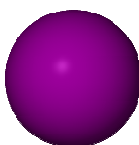
Atomic Colour Key

Colour

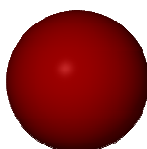
Element



Metal



Sulphur



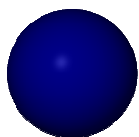
Oxygen



Carbon



Hydrogen



Nitrogen



Chlorine/bromine

Glossary of Terms

1-D	One dimensional
2-D	Two dimensional
3-D	Three dimensional
α	angle between the b and c axes
β	angle between the a and c axes
γ	angle between the a and b axes
ATR	Attenuated Total Reflection
CIF	Crystallographic Information File
CPK	Corey-Pauling-Koltun
CSD	Cambridge Structural Database
DNA	Deoxyribonucleic Acid
FTIR	Fourier-Transform Infrared
LC ESI-MS	Liquid Chromatography Electrospray Ionisation Mass Spectrometry
MOF	Metal Organic Framework
NMR	Nuclear Magnetic Resonance
PXRD	Powder X-ray Diffraction
RNA	Ribonucleic Acid
SCD	Single-Crystal Diffraction
Z	Number of formula units in the unit cell

Chapter 1

Crystal Engineering

1.0 Introduction

Crystal engineering is a young and emerging field of science encompassing chemistry and materials science.¹ Put in very simple terms crystal engineering can be defined as “*making crystals by design*”.² The process of crystal synthesis is analogous to retrosynthetic analysis in molecular synthesis.³ In crystal engineering, the crystal is the retrosynthetic target,³ whose fundamental building block is called a *tecton*^{4,6} and the retrosynthetic analysis gives rise to smaller units called *supramolecular synthons*.^{3,7} Supramolecular synthons can be thought of as playing the same role as that of *synthons* in molecular chemistry.³ Therefore the process of crystal synthesis involves the *self assembly* of tectons *via intermolecular interactions* (Figure 1.1).

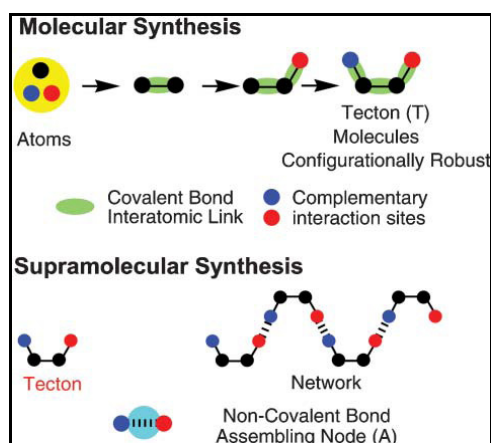


Figure 1.1. Comparison between molecular synthesis and supramolecular synthesis⁵.

The term *crystal engineering* was first introduced by Pepinsky⁸ in 1955 in relation to the exploitation of complex ions in structure determination of optically active ions. Twenty years later, Schmidt implemented the term in connection with photodimerisation of cinnamic acid.⁹ In recent times, the term has broadened and is now being used for the supramolecular synthesis of inclusion compounds, co-crystals and coordination polymers.¹⁰ A formal definition of crystal engineering was given by Desiraju who defined the term as “...*the understanding of intermolecular interactions in the context of crystal packing and in the utilization of such understanding in the design of new solids with desired physical and chemical properties*”.¹¹ The first part in this chapter discusses *tectons*, *supramolecular*

synthons, intermolecular interactions and *self assembly*, their relationships to one another and their role in crystal engineering. The second part discusses coordination polymers, a class of crystal engineered materials.

1.1 Tectons and supramolecular synthons

Tectons

Tectons are the fundamental building blocks in crystal engineering which bear within their structures intermolecular recognition sites that enable them to recognize one another and to self assemble at the molecular level.^{5,6,12} The recognition pattern between complementary tectons is known as the assembling node⁵ or supramolecular synthon if it is reliable and predictable.³ The recognition pattern may contain any one of the following intermolecular interactions: hydrogen bonding, van der Waals, electrostatic, π - π and coordination bonding.¹²

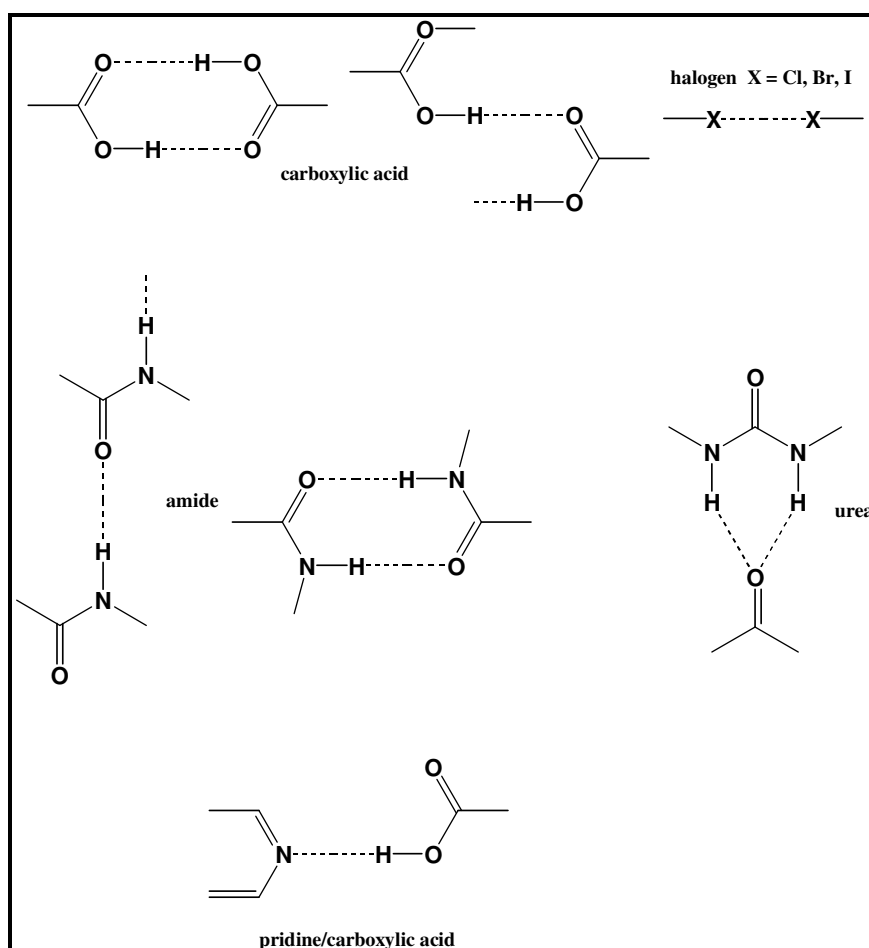
Supramolecular synthons

The main obstacle in crystal engineering is the lack of synthetic control over the final crystalline solid.¹³ In molecular synthesis, reactions have been discovered and refined, thus allowing synthesis of target molecules.^{14,15} In this regard, crystal engineering is far from reaching a level where target crystals can be synthesized at will.¹⁴ Because of the lack of synthetic control, it is difficult to predict how the building blocks will assemble in the solid state. The problem of crystal structure prediction may also be attributed to the weak intermolecular interactions holding molecules together in the solid state, as these are numerous and non-directional. As a result numerous free energy minima are possible within the global minima.^{5,16} Indeed, this phenomenon explains the occurrence of polymorphism and pseudopolymorphism in solid state structures.¹⁷ Crystal engineers are generally concerned with finding a synthetic strategy that will provide synthetic control over crystalline solids, thus enabling them to tailor crystals with desired functions.^{13,14}

A variety of synthetic strategies for crystal engineering including computational and experimental approaches, have been proposed. One of the most recognized strategies is the concept of supramolecular synthons, which was introduced by Desiraju in 1995.³ This concept is based on analyzing existing crystal structures for certain repetitive units between the same functional groups and intermolecular interactions.¹⁸ The repetitive units have been termed supramolecular synthons and are formally defined as “*structural units within supermolecules which can be formed and/or assembled by known or conceivable synthetic operations involving intermolecular interactions*”.³ A supramolecular synthon is not to be

confused with an intermolecular interaction. The latter is a fundamental part of the supramolecular synthon and is thus the “functional group”. It is the geometrical and chemical features of its components that distinguish a supramolecular synthon from an intermolecular interaction.³ Crystal engineering relies on the robustness of the supramolecular synthons to predictably assemble building blocks in the solid state, much like covalent bond formation in molecular synthesis.

Although supramolecular synthons involving all intermolecular interactions are known, the most commonly occurring involve hydrogen bonds. The supramolecular synthons are subdivided into (i) homosynthons, which are a result of interactions between identical complementary functional groups, e.g. amide dimers and carboxylic acid dimers,¹⁰ and (ii) heterosynthons, which are a result of interactions between complementary but different functional groups e.g. hydroxyl and aromatic nitrogen.¹⁰ Some of the common supramolecular synthons are shown in Scheme 1.1



Scheme 1.1. Some common supramolecular synthons.^{3,10}

1.2 Intermolecular interactions

One of the main goals of crystal engineering is to understand intermolecular interactions and to apply this knowledge in the synthesis of new materials with desired properties.¹ Intermolecular interactions can be classified as (i) directional or (ii) non-directional forces.³ Also referred to as long range interactions, “directional interactions form between heteroatoms N, S, O, Cl, Br, I, (rarely B, F, P, Se) or between any one of the heteroatoms and either C or H.”³ On the other hand, non-directional forces, also known as medium range forces involve the van der Waals interactions and these are among the weakest interactions with their strength ranging between 0.5 and 2 kcal/mol.⁵

1.2.1 Directional forces

The hydrogen bond

The hydrogen bond is by far the most frequently occurring interaction dominating organic crystals and the structures of biological systems such as the nucleic acids, proteins and polysaccharides.¹⁹ The hydrogen bond interaction was first identified in the 1920s by Latimer and Rodebush who suggested that “*a free pair of electrons on one water molecule might be able to exert sufficient force on a hydrogen held by a pair of electrons on another water molecule to bind the two water molecules together.*”²⁰ This was followed by the study of Pimentel and McClellan in 1960 in which they examined 2000 cases where hydrogen bonding existed.²¹ Based on this study the authors first defined hydrogen bonding by stating that “*a hydrogen bond exists if (1) there is evidence of a bond and (2) there is evidence that this bond sterically involves a hydrogen atom already bonded to another atom.*”²¹ According to Steiner, this definition cannot be accepted fully as it does not specify the chemical nature of the atoms and the interaction geometry.²² A modified definition of the hydrogen bond was later presented by Steiner in 2002 and it states that: “*an X—H·····A interaction is called a hydrogen bond if (1) it constitutes a local bond, and (2) X—H acts as proton donor to A.*”²²

The X—H·····A (X = donor and A = acceptor) bond is defined by the geometric parameters d , D , r , θ and ϕ as shown in Figure 2.²² Hydrogen bonding interactions can be divided into three categories based on their strength: (i) very strong (ii) strong and (iii) weak hydrogen bonds.²³ Detailed characteristics of the three categories of hydrogen bonds are given in Table 1.1. Normally, one donor would interact with one acceptor (Figure 1.2a), but in some cases, because of the long range nature of the hydrogen bond, the donor may interact with two

or three acceptors at the same time (Figure 1.2b, c). In such instances, the hydrogen bond is termed bifurcated and trifurcated, respectively²³.

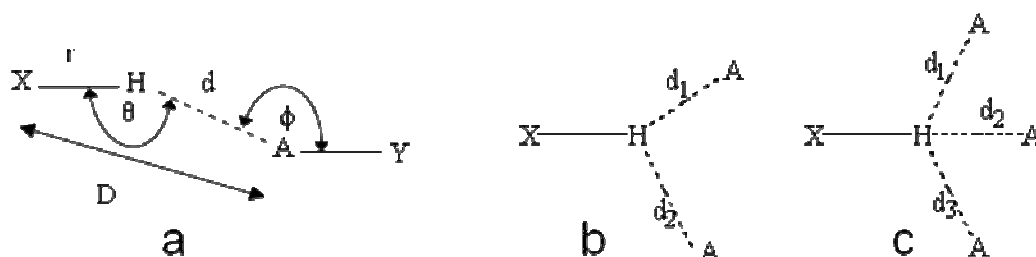


Figure 1.2. (a) The definition of the geometric parameters for a hydrogen bond, (b) bifurcated and (c) trifurcated hydrogen bond.²³

Table 1.1. Characteristics of very strong, strong and weak hydrogen bonds.²³

	Very Strong	Strong	Weak
Interaction type	Strongly covalent	Mostly electrostatic	Electrostatic/dispersive
Bond energy (-kcal/mol)	15-40	4-15	<4
Examples	[F...H...F] ⁻ [N...H...N] ⁺ P-OH...O=P	O-H...O=C N-H...O=C O-H...O-H	C-H...O O-H...π Os-H...O
Bond lengths	X-H ≈ H...A	X-H < H...A	X-H << H...A
Lengthening of X-H [Å]	0.08-0.25	0.02-0.08	<0.02
D(X...A) [Å]	2.2-2.5	2.5-3.2	>3.2
d(H...A) range [Å]	1.2-1.5	1.5-2.2	>2.2
Bonds shorter than the van der Waals radii	100%	Almost 100%	30- 80%
θ(X-H...A) range (°)	170-180	>130	>90
Effect on crystal packing	Strong	Distinctive	Variable
Utility in crystal engineering	Unknown	Useful	Partly useful
Interaction type	Strongly covalent	Mostly electrostatic	Electrostatic/dispersive
Electrostatics	Significant	Dominant	Moderate
Directionality	Strongly	Moderate	Weak

The coordination bond

The coordination bond is the strongest (30-70 kcal/mol) of all intermolecular interactions and offers greater directionality and stability than the other intermolecular interactions.⁵ A coordination bond forms between a labile metal ion with a vacant site and a ligand that is capable of donating a lone pair of electrons.⁵ The coordination bond has been successfully applied in crystal engineering in designing materials known as coordination polymers.²⁴ These are discussed in much more detail later in the chapter.

1.2.2 Non-directional forces

Non-directional forces are the weakest intermolecular interactions. These forces are generally due to C \cdots C, C \cdots H and H \cdots H interactions.³ Non-directional forces influence the packing, shape and size of a molecular crystal structure and this influence is dependent upon the C:H stoichiometric ratio.³ In the case of high C:H ratios, aromatic compounds usually interact *via* three types of interactions, i.e. the stacked, offset and the edge-to-face (T-shaped herringbone).^{3,10} The stacked and offset motifs result from stacking of the rings as a way of increasing the C \cdots C interactions.³ C \cdots H type interactions are encountered when the aromatic rings are arranged in an edge-to-face motif or the T-shaped herringbone motif with a van der Waals separation of 3.3-3.8 Å.^{3,10} The three types of interactions are shown in Figure 1.3.

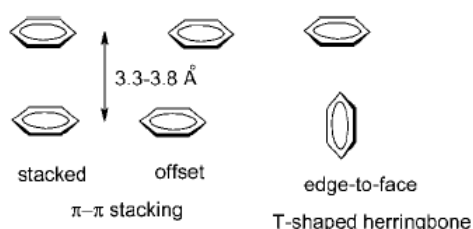


Figure 1.3. Three types of interactions possible between phenyl rings.¹⁰

1.3 Self assembly

Whitesides defined self assembly as a process in which components, either separate or linked, spontaneously form ordered aggregates.²⁵ A much simpler definition is given by Palesko who referred to the process as the “*science of things that put themselves together*”.²⁶ The process of self assembly is scientifically interesting because it is responsible for the assembly of nature’s complex structures i.e. the lipid membranes, folded proteins and protein aggregates.²⁵ In crystal engineering, molecular networks are generated *via* the self assembly process, involving millions of tectons.⁵ For the process of self assembly to be successful a system must possess the following characteristics:

- The system must contain like or unlike components that are able to interact with one another to form an ordered and thermodynamically stable final state.²⁵ These components must be complementary to one another;
- The interactions between the molecules must be weak and reversible, this would allow the system to self repair if mistakes are generated.⁵

The process of self assembly can result in discrete, 1-D, 2-D or 3-D networks. The relationship between tectons, supramolecular synthons and self assembly is illustrated in Figure 1.4.

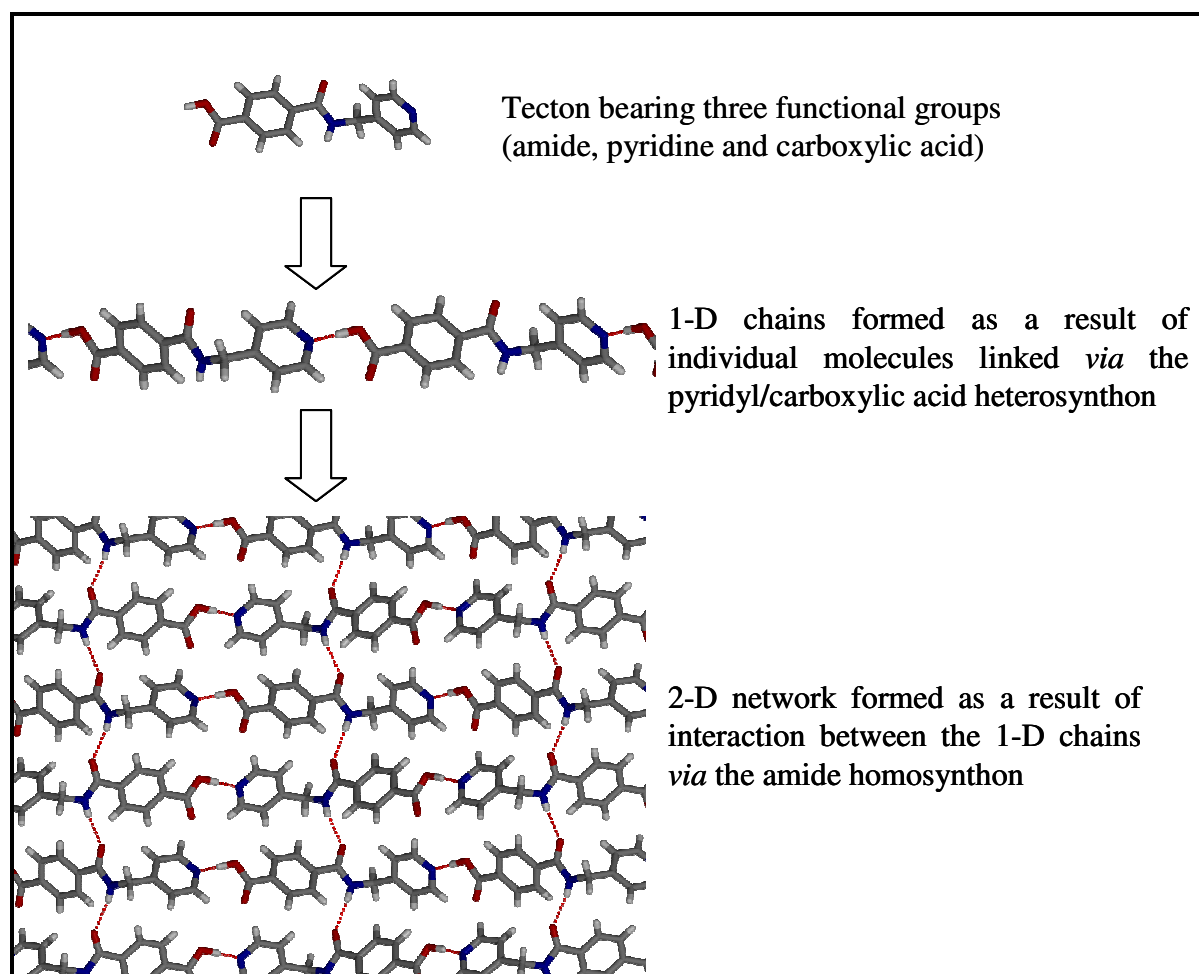


Figure 1.4. Generation of a 2-D network *via* self assembly of 4-(pyridin-4-ylmethyl)aminocarbonyl benzoic acid. The individual molecules interact *via* the pyridine/carboxylic acid heterosynthon as well as the amide homosynthon.[#]

Discrete assembly: According to Lauher, discrete assemblies are supramolecular complexes that lack translational symmetry. Discrete units are finite and are defined by the point group symmetry; they may be symmetrical, i.e. they may possess the C_i point group symmetry, or may be asymmetric, in which case they possess no symmetry elements.²⁷ *1-D or α -networks:* 1-D or α -networks possess translational symmetry in one direction and these are defined by the rod group symmetry. 1-D networks may be composed of a single tecton, or a combination of different tectons that can generate two diverging recognition sites. The

[#]4-(pyridin-4-ylmethyl)aminocarbonyl benzoic acid was synthesized during the course of this study. The synthetic method and crystal structure are described in detail in Chapters 2 and 3, respectively.

presence of the diverging sites prevents the formation of discrete units. A 1-D network may also consist of discrete units that are related by translational symmetry.²⁷ *2-D or β -networks:* 2-D networks possess three degrees of translational symmetry, and they are defined by their layer group symmetry. 2-D networks may consist of discrete units or α -networks as substructures. They should each possess at least three diverging recognition sites.²⁷ *3-D or γ -networks:* 3-D networks possess three degrees of translational symmetry and may contain 1-D networks or 2-D networks as substructures. 3-D networks are defined by their space group symmetry.²⁷

1.4 Coordination polymers

Coordination polymers are synthesized by reacting a carefully designed tecton (hereafter referred to as a ligand) with a labile metal ion.²⁴ The most commonly used labile metal ions include Cu^+ , Cu^{2+} , Cd^{2+} , Zn^{2+} , Co^{2+} and Ni^{2+} .²⁴ Crystal engineering of coordination polymers utilizes diverging polydentate ligands with two or more donor atoms.^{2,28} The ligands are termed ditopic, tritopic and tetratopic, depending on the number of donor atoms.²⁸ The nitrogen and oxygen donor ligands are the most widely used ligands in the construction of coordination polymers. The polydentate ligands act as a bridge between metal centres and allow the network to propagate in 1-D, 2-D and 3-D.²⁴ This is illustrated in Figure 1.5. The overall structure of the coordination polymer is dependent upon a number of factors such as the metal to ligand ratio,²⁹ the solvent system,³⁰ the coordination geometry of the metal,^{24,31} the nature of the ligand,³² and the nature of the counterion.³³ In addition, weak interactions also play a key role as these are numerous, weak and non directing.²⁸ Other less obvious factors such as the crystallization methods, the temperature of the system and the concentration of reactants also have an influence on the final crystal structure.²⁸

One of the main motives behind the synthesis of coordination polymers is to make zeolite-type materials that contain channels or voids that can absorb and release small molecules.^{2,34} Such coordination polymers are popularly known as metal organic frameworks (MOFs).³⁴ MOFs have found wide applications in new chemical separations and gas storage.² Two main challenges are encountered in MOF synthesis.

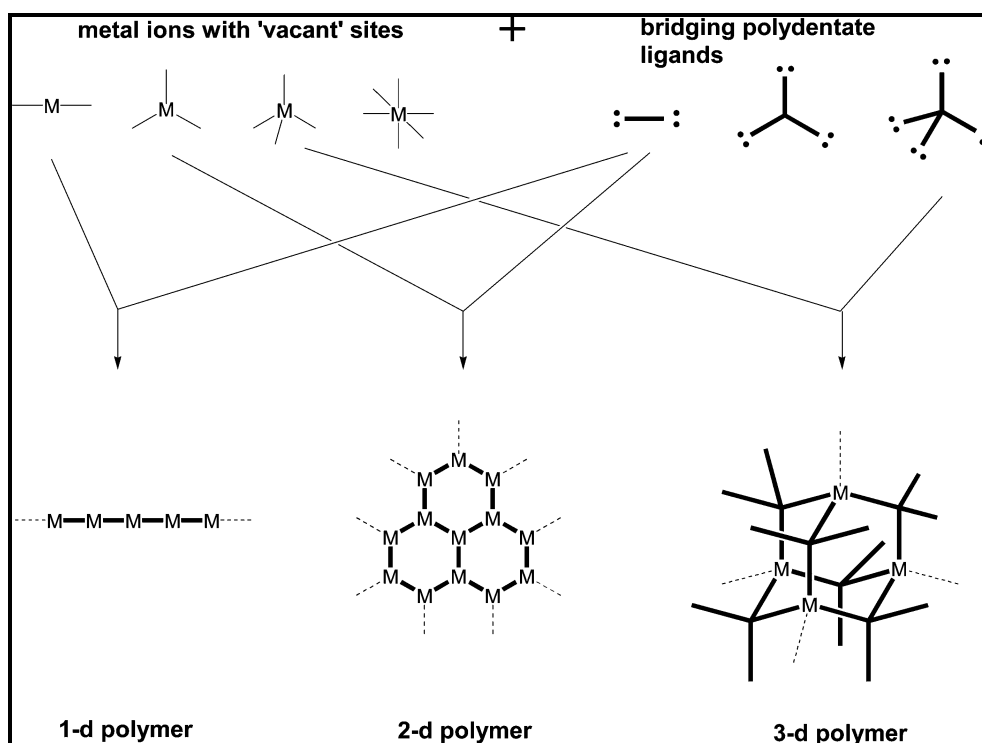


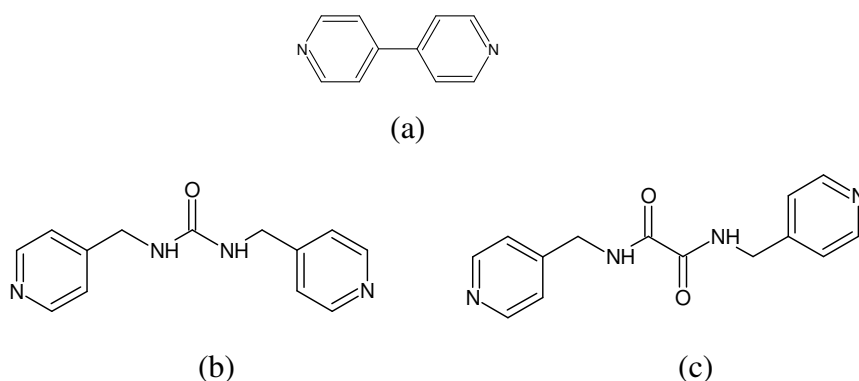
Figure 1.5. Three types of networks that can be constructed using polydentate ligands and metal ions.²⁴

First, in some cases the self assembly process of metal organic frameworks can leave voids or channels that are occupied by solvent molecules while, in other cases, one polymer network may interpenetrate the other thereby filling up potential cavities.³⁵ Secondly, even if interpenetration does not occur, the framework might not survive the process of guest removal.² Therefore, MOF synthesis focuses on understanding the factors that control interpenetration as well as designing robust frameworks that can withstand the process of guest removal.²

Yaghi and co-workers have been most effective in designing a synthetic strategy that yields robust frameworks.³⁴ This synthetic strategy is known as reticular synthesis and utilizes metal carboxylate instead of the single metal ions.³⁴ The carboxylate locks the metal into a specific geometry and the carboxylate carbon forms the point of extension, which offers directionality. These points of extension are referred to as secondary building units (SBUs) and they impart rigidity to the framework. By using this strategy, Yaghi and other groups have managed to synthesize frameworks that are robust and exceptionally stable upon guest removal.^{34,36}

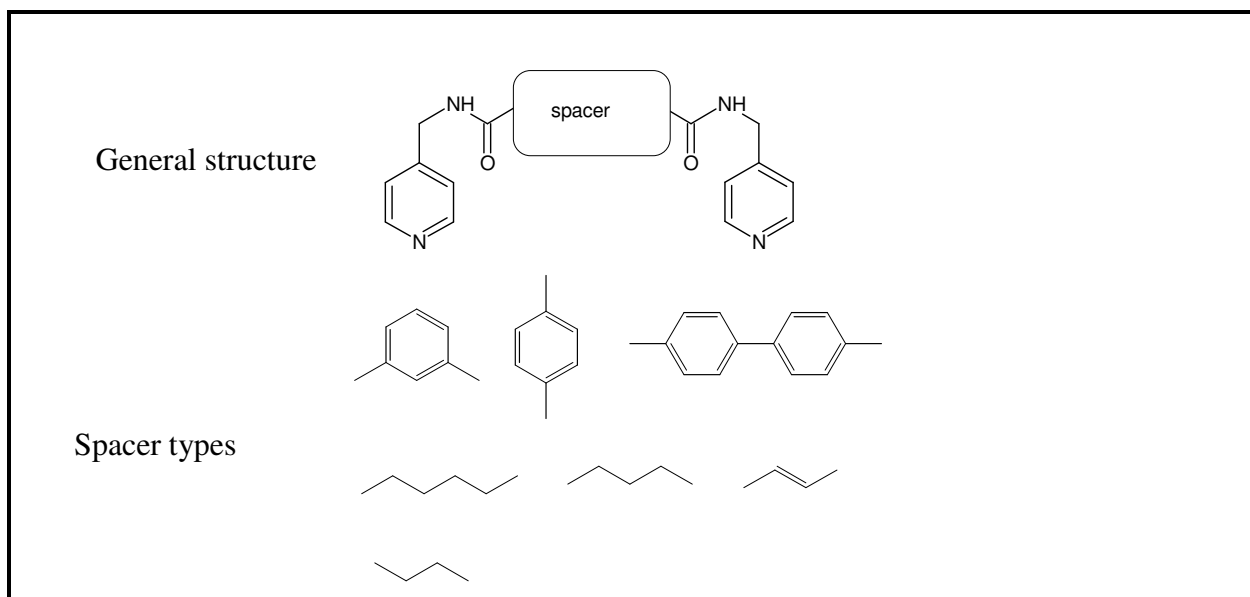
1.4.1 Coordination complexes of ligands containing the bis-pyridyl and amide functionalities

Bipyridine is one of the most widely used ligands in the construction of coordination polymers³⁷⁻³⁹ (Scheme 1.2). Coordination compounds that feature this ligand have been shown to possess properties such as porosity, magnetism and conductivity.²⁸ Derivatives of the bipyridine ligands, consisting of various kinds of spacer units between the pyridine rings have also been utilized in the design of 1-D, 2-D and 3-D networks.²⁸ One class of compounds that has been studied in the past years contains the oxalamide or the urea group as the spacer unit^{40,41} (Scheme 1.2). Studies of this class of compounds have mainly focused on co-crystallization with other compounds containing the carboxylic acid moiety. An important finding of these studies was that ureas and oxalamides are capable of assembling into α -networks *via* self-complementary hydrogen bonds⁴¹ and that these interactions are persistent even when the ligands are co-crystallized with compounds containing carboxylic acid.⁴⁰ Coordination complexes that feature these ligands have only been reported recently.^{33,42-44}



Scheme 1.2. (a) The bipyridine ligand and bis-pyridyl based ligands containing (b) the urea or (c) oxalamide functionalities.

A similar class of compounds that has received considerable attention over the past decade is that of compounds containing the bipyridine unit and the amide functionality (Scheme 1.3). The first ligand of this type appeared in the literature in 1998,⁴⁵ and since then the number of reports featuring these ligands have increased dramatically. A review of the literature indicates that coordination complexes consisting of these ligands possess structural features such as helicity,^{46,47} water clusters^{45,48,49} and porosity⁵⁰ and some of these properties are discussed in the next section.



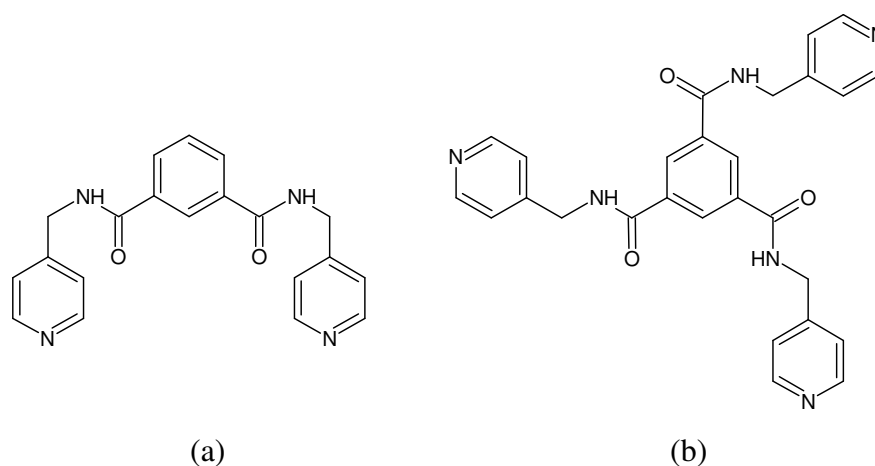
Scheme 1.3. The general structure of bis-pyridyl diamide ligands and the various spacers

1.4.2 Properties of coordination complexes of bis-pyridyl diamide ligands

Water clusters

One of the interesting properties of bis-pyridyl based ligands is their high affinity for water.⁴⁵ The coordination complexes of these types of ligands have been shown to encapsulate water clusters of the type $(\text{H}_2\text{O})_n$ ^{45,48,49} Much research effort has centred on the study of pure water clusters as this may be key to understanding the anomalous behaviour of water.^{49,51} It is also known that water clusters play an important role in stabilizing the structure of proteins such as carbonic anhydrase C⁵² and actidin.⁵³

N,N'-bis(pyridine-4-ylmethyl)isophthalamide (**ISO**) was the first ligand consisting of a bis-pyridyl moiety and an amide functionality to be presented in the literature (Scheme 1.4).⁴⁵ Reaction of **ISO** with either $\text{Cu}(\text{NO}_3)_2$ ⁴⁵ **1** or $\text{Co}(\text{NO}_3)_2$ ⁴⁸ **2** in water resulted in a 0-D dinuclear cage-like complex $[\text{M}_2(\text{ISO})_4(\text{H}_2\text{O})_4](\text{NO}_3)_4 \cdot 16\text{H}_2\text{O}$. Complex **1** crystallizes in the tetragonal space group $I4_1/a$ while complex **2** crystallizes in the monoclinic space group $C2/c$. In both structures the metal centres are linked by means of four bridging ligands to form a 0-D cage-like complex. The M^{2+} cation, which adopts an octahedral geometry, is coordinated to four ligands *via* the pyridyl nitrogen atom and two water molecules. The cages stack in linear arrays with the $\text{M} \cdots \text{M}$ axes parallel to $[001]$. Adjacent arrays are staggered, leaving cavities that contain a discrete hydrogen bonded water cluster H_2O_{10} (Figure 1.6a) which is very similar to the smallest subunit of ice I_c (Figure 1.6b). The $\text{O} \cdots \text{O}$ distances (average length, 2.80(5) Å) of the water cluster are comparable with the $\text{O} \cdots \text{O}$ distances (2.75 Å) of ice.



Scheme 1.4. (a) **ISO**, the first ligand containing an amide functionality and bis-pyridine moiety to be presented in the literature, (b) Tritopic ligand **BEN**

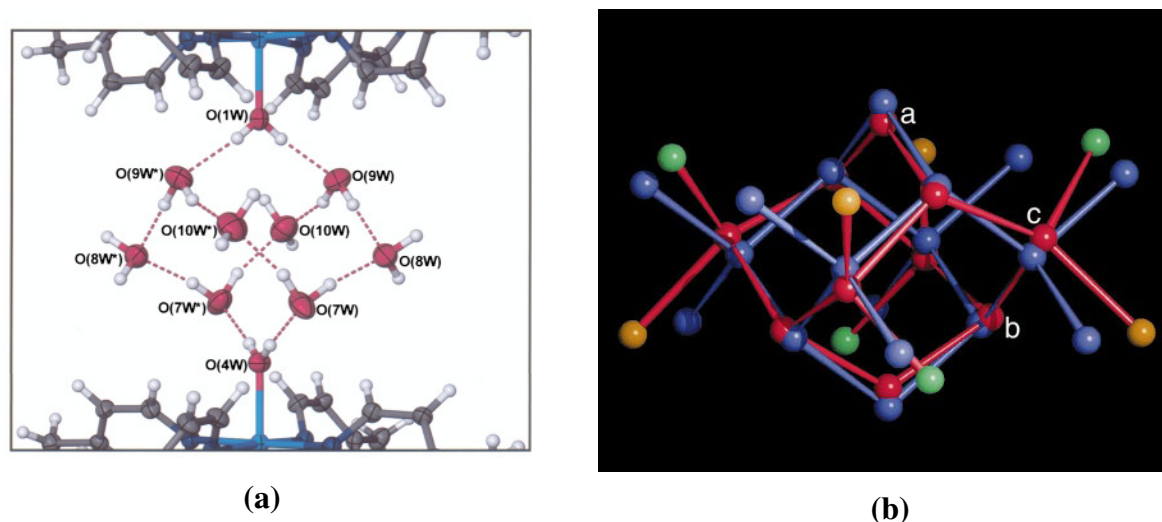


Figure 1.6. (a) The $(\text{H}_2\text{O})_{10}$ water cluster in **1** and (b) comparison between the water cluster (red) and ice Ic (blue). The three unique water molecules are labelled a, b and c.^{45,48}

The water cluster is believed to stabilize the molecular cages by efficiently occupying the cavity as well as connecting successive cages. The structure is further stabilized by eight types of hydrogen bonds between the water cluster and the nitrate anions of adjacent cages. The water cluster in the two complexes differ in the distance between O(1W) and O(4W). The distance between O(1W) and O(4W) in complex **1** is 5.779(7) Å while the corresponding distance in complex **2** is 6.287(4) Å. The difference in the distances was attributed to the longer Cu–O bond (average Cu–O bond 2.33 Å and average Co–O 2.10 Å) in complex **1**. Despite the difference in distances between O(1W) and O(4W), the water clusters are similar. This demonstrates that a change in the geometry of the metal centre does not significantly change the overall conformation of the water cluster. The water cluster is quite flexible and robust.

Another interesting water cluster was reported by Wang *et al.*⁴⁹ In their study they crystallized the ligand *N,N,N'*-tris(pyridin-4-ylmethyl)-1,3,5-benzenetricarboxamide (**BEN**) (Scheme 1.4), which has a tripyridyl moiety, with $\text{Cu}(\text{BF}_4)_2 \cdot 6\text{H}_2\text{O}$ in CH_3NO_2 and CH_3OH . This resulted in a novel $\text{M}_6(\text{BEN})_8$ 0-D cage (Figure 1.7a) which crystallizes in the tetragonal space group $I432$. The cage encapsulates two novel $(\text{H}_2\text{O})_{56}(\text{OH})_6$ and $(\text{H}_2\text{O})_{20}$ water clusters in its cavity (Figures 1.7b and 1.8). The two water clusters were further classified as inner and outer water clusters. The $(\text{H}_2\text{O})_{56}(\text{OH})_6$ entity forms the outer cluster with a large cavity in which the inner $(\text{H}_2\text{O})_{20}$ cluster is encapsulated as a guest. The water clusters are stabilized by hydrogen bonding between the coordinated hydroxyl anions and the water molecules.

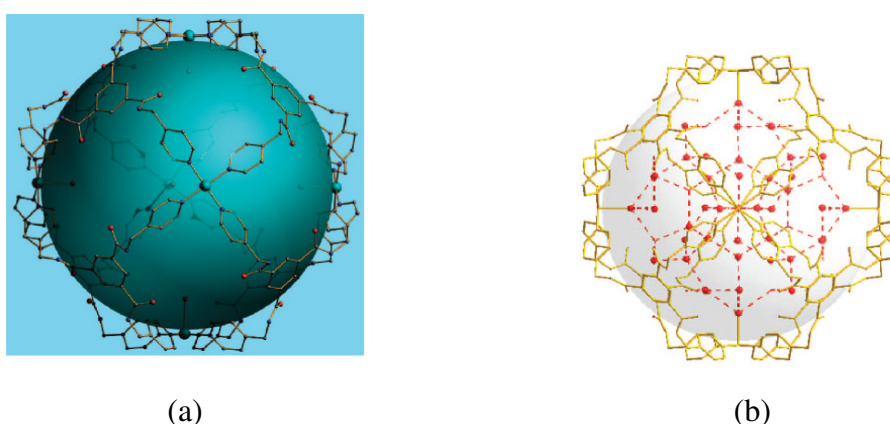


Figure 1.7. (a) The $\text{M}_6(\text{BEN})_8$ cage and (b) the $\text{M}_6(\text{BEN})_8$ cage as well as the outer and inner water clusters.⁴⁹

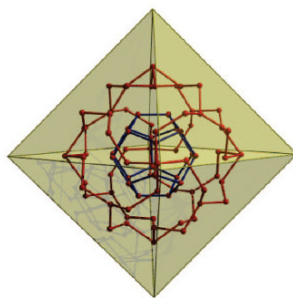
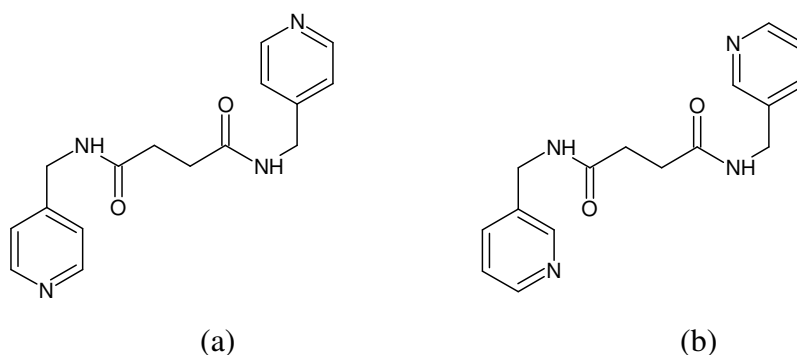


Figure 1.8. Schematic diagram the $\text{M}_6(\text{BEN})_8$ cage. The pale yellow octahedron represents the $\text{M}_6(\text{BEN})_8$ cage. The inner and outer clusters are shown in blue and red, respectively.⁴⁹



Scheme 1.5. Isomeric ligands (a) **SUC-1** and (b) **SUC-2**.

Helicity

Coordination compounds that possess helicity are interesting because they mimic nature's self assembly processes, i.e. the DNA double helix, RNA and the peptide chain α -helix.⁴⁷ Isomeric ligands *N,N'*-bis(pyridin-4-ylmethyl)butanediamide (**SUC-1**) and *N,N'*-bis(pyridin-3-ylmethyl)butanediamide (**SUC-2**) (Scheme 1.5) have been shown to yield helical complexes.^{46,47} Reaction of **SUC-1** with $\text{Cd}(\text{NO}_3)_2$ and succinic acid in a mixture of DMF and water yielded the novel coordination polymer $\{[\text{Cd}(\text{succinate})(\text{SUC-1})]\cdot\text{H}_2\text{O}\}_n$ comprising both single and triple helices.⁴⁶ The triple helix is formed by three interwoven **SUC-1** molecules while the single helix is formed by the succinic acid molecule (Figure 1.9).

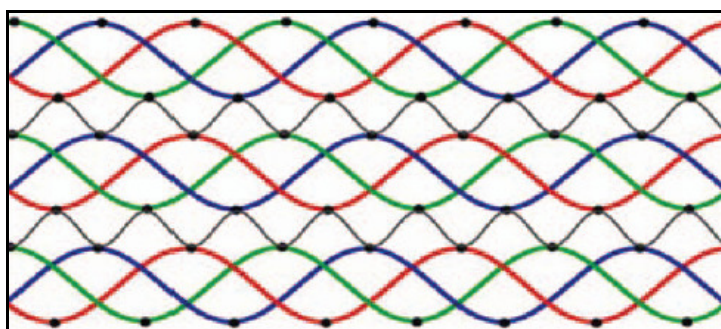


Figure 1.9. Schematic diagram showing single (black) and triple (red, blue and green) helices in $\{[\text{Cd}(\text{succinate})(\text{SUC-1})]\cdot\text{H}_2\text{O}\}_n$. The triple helix is formed by three interwoven **SUC-1** molecules while the single helix is formed by the succinic acid molecule. The metal centres are shown as black circles.⁴⁶

Reaction of **SUC-2** with CuClO_4 in ethanol yielded a novel double helical coordination network with shared copper atoms.⁴⁷ The helical chains are composed of $\text{Cu}(\text{SUC-2})_2(\text{H}_2\text{O})_2$. The Cu centres are linked by bridging **SUC-2** molecule to form 1-D strands which are entwined forming a double helix, where the two strands cannot be pulled apart independently (Figure 1.10).

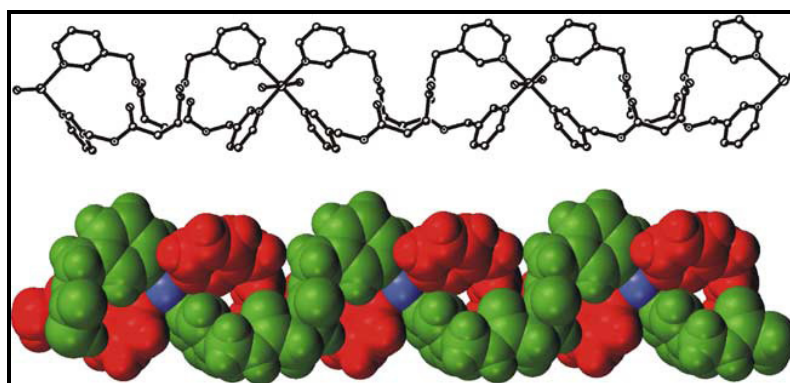


Figure 1.10. The double helix as well as the space filling model of $\{[\text{Cu}(\text{SUC-2})_2(\text{H}_2\text{O})_2]\}_n$. The strands of the double helix are coloured in green and red to distinguish them from each other.⁴⁷

Isomeric ligands

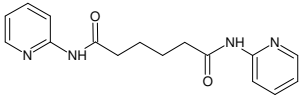
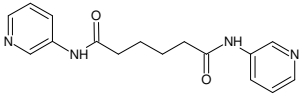
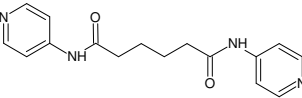
The substitution position of the pyridine ring can be varied from 2 to 3 and 4. It is therefore interesting to study the coordination abilities of ligands with different donor atom positions. One such study was carried out by Hsu *et al.*⁵⁴ who designed and prepared three ligands, *N,N'*-dipyridin-2-ylhexanediamide (**L1**), *N,N'*-dipyridin-3-ylhexanediamide (**L2**) and *N,N'*-dipyridin-4-ylhexanediamide (**L3**). Reactions of these ligands with Cd(ClO₄)₂·6H₂O in ethanol yielded 1-D (complex **3**), 2-D (complex **4**) and 3-D (complex **5**) coordination polymers.

Complex **3** crystallizes in the monoclinic space group $P2_1/n$. The cadmium centre adopts a distorted octahedral geometry and is coordinated to two pyridyl nitrogen atoms, two carbonyl oxygen atoms of two unique ligands and two oxygen atoms of the two perchlorate anions. The ligand, which coordinates in a tetradentate fashion, links metal centres to form 1-D zigzag chains which interact *via* extensive hydrogen bonding between the coordinated perchlorate anions and the amide NH group ($N-H\cdots O = 2.203 \text{ \AA}$) to form a 3-D network.

Complex **4** crystallizes in the triclinic space group $P\bar{1}$. The metal centres are linked by a single bridging **L2** ligand to form a 2-D pleated network. These 2-D nets interact *via* hydrogen bonding between the amide NH and the perchlorate anion ($N-H\cdots O = 2.044 \text{ \AA}$).

Complex **5** crystallizes in the orthorhombic space group $Pcca$. The structure consists of 2 independent **L3** ligands which link the metal centres to form a 3-D interpenetrated network. In contrast to complex **4**, the ligands adopt two distinct conformations; anti-anti-anti (AAA) and anti-gauche-anti (AGA). The conformations are given by the $sp^3 C-C-C-C$ torsion angles, G is defined as $180 \geq \theta \geq 90$ and A is defined as $0 \leq \theta \leq 90$. A detailed comparison of the three complexes is given in Table 1.2. To summarize, Cd complexes of the three isomeric ligands **L1**, **L2** and **L3** were synthesized and the complexes form 1-D zigzag, 2-D pleated and 3-D interpenetrated coordination complexes, respectively. **L1** behaves as a tetradentate ligand in complex **3** while **L2** and **L3** are bidentate. **L3** can adopt two conformations AAA and AGA. These results clearly show that the position of the donor atom on the pyridine ring can greatly influence the nature of the coordination complex that forms.

Table 1.2. Comparison of the three complexes **3-5**

Ligand	 L1	 L2	 L3
Complex	3	4	5
Space group	$P2_1/n$	$P\bar{1}$	$Pcca$
Metal centre coordination environment	(i) Metal centre adopts distorted octahedral geometry (ii) Coordinated to two nitrogen and two oxygen atoms of two L1 ligands (iii) Coordinated to two oxygen atoms of two perchlorate anions.	(i) Metal centre adopts octahedral geometry (ii) Coordinated to four pyridyl nitrogen atoms of four L2 ligands (iii) Coordinated to two oxygen atoms of two methanol molecules	(i) Metal centre adopts octahedral geometry (ii) Coordinated to four pyridyl nitrogen atoms of four L3 ligands (iii) Coordinated to two oxygen atoms of two methanol molecules
Conformation	AAA	GAG	AAA, AGA
Dimensionality	1-D zigzag chain	2-D pleated network	3-D interpenetrated network
Coordination mode of ligand	Tetradentate	Bidentate	Bidentate

1.5 Aims and objectives

The aims of this study were:

- To synthesize *N*-donor ditopic ligands containing the amide functionality as well the bis-pyridyl moiety;
- To crystallize the ligands with different metal salts varying the following parameters: the metal to ligand ratio, the solvent system and the nature of the counterion;
- To study the self assembly process of the crystalline products.

These ligands are particularly interesting to study for several reasons:

- The ligands are relatively easy to synthesize and a wide range of spacer types can be utilized;
- The donor atom position on the pyridine ring can be varied from 2 to 3 and 4, thus coordination abilities of isomeric ligands can be studied;
- The ligands contain the amide functionality, which can act as both a hydrogen bond donor and acceptor *via* self-complementary amide hydrogen bonds (amide homosynthon). It would be interesting to determine whether the interaction persists in the presence of other competing species such as solvent molecules and metal counter ions;
- The rigid pyridine rings and the phenyl rings (in some ligands) can participate in

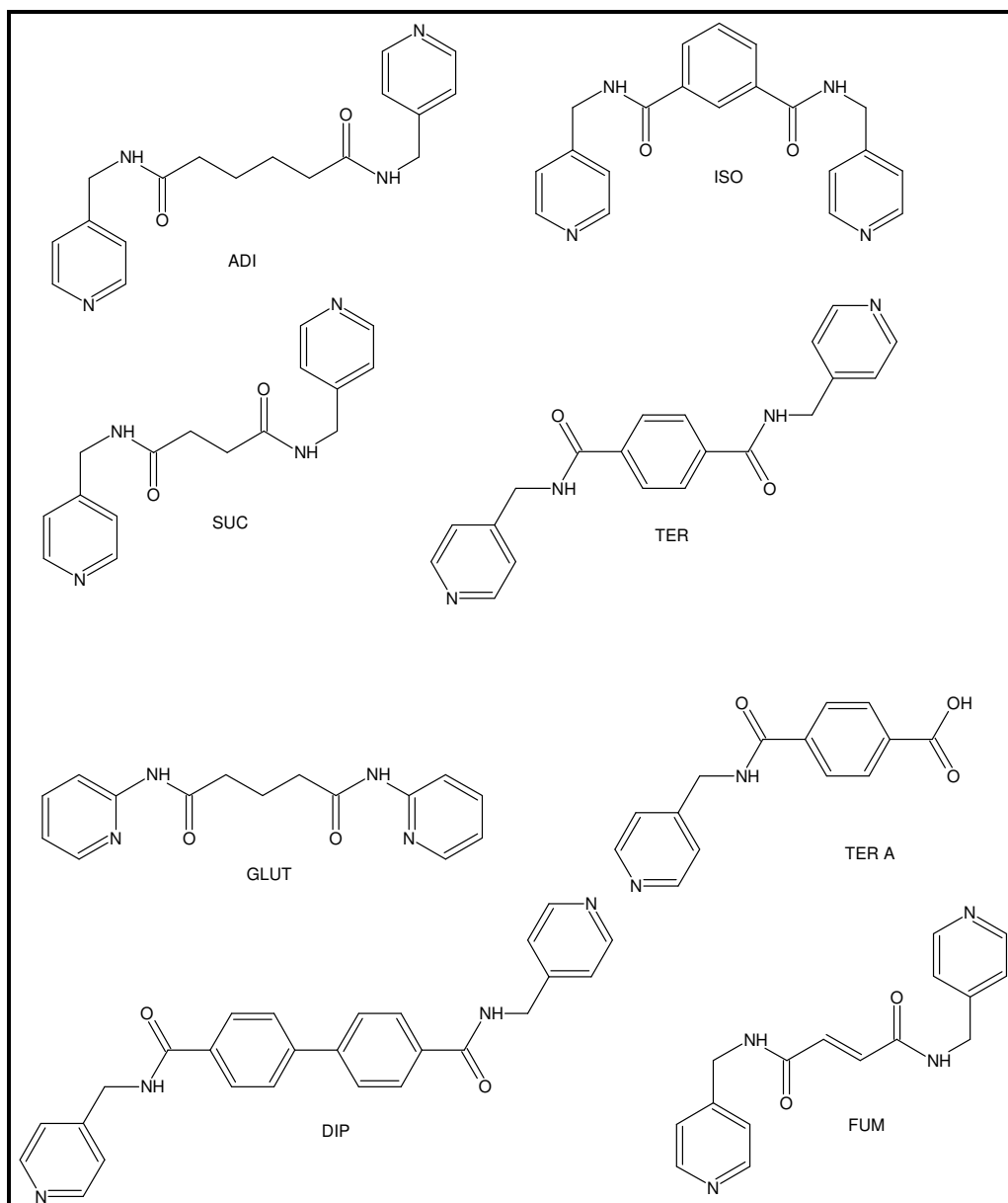
π - π stacking which could add complexity to the structure;

- Ligands of this type have been shown to yield complexes with interesting structural features (Section 1.16).

To this end, we synthesized eight structurally related ditopic ligands namely,

- *N,N'*-bis(pyridin-4-ylmethyl)isophthalamide (**ISO**);
- *N,N'*-bis(pyridyl-4-ylmethyl)terephthalamide (**TER**);
- *N,N'*-bis(pyridin-4-ylmethyl)hexanediamide (**ADI**);
- *N,N'*-bis(pyridin-4-ylmethyl)butanediamide (**SUC**);
- *N,N'*-bis(pyridin-4-ylmethyl)biphenyl-4,4'-dicarbonyl dicarboxamide (**DIP**);
- *N,N'*-dipyridin-2-ylpentanediamide (**GLUT**);
- (*2E*)-*N,N'*-bis(2-pyridin-4-ylmethyl)but-2-enediamide (**FUM**);
- 4-(pyridin-4-ylmethyl)aminocarbonyl benzoic acid (**TER-A**).

Of these, **ADI**, **DIP**, **GLUT** and **TER-A** are novel whilst the other four have been reported in the literature either in their pure form or in metal organic complexes. All of these ligands, except **TER-A** and **GLUT** possess the 4-(aminomethyl)pyridine moiety. **GLUT** has the 2-aminopyridine moiety while **TER-A** has a 4-(aminomethyl)pyridine moiety and a carboxylic acid moiety. The general structures of the ligands are shown in Scheme 1.6.



Scheme 1.6. Eight structurally related ditopic ligands synthesized for this study.

1.6 References

1. L. Brammer, N. R. Champness and D. Braga, *CrystEngComm*, 2005, **7**, 1.
2. D. Braga, *Chem. Commun*, 2003, 2751.
3. G. R. Desiraju, *Angew. Chem. Int. Ed. Engl.*, 1995, **34**, 2311.
4. D. S-M. Simard and J. D. Wuest, *J. Am. Chem. Soc.* 1991, **113**, 4696.
5. M. W. Hosseini, *CrystEngComm*, 2004, **6**, 318.
6. P. Metrangolo and G. Resnati, *Encyclopedia of Supramolecular Chemistry*, 2004, **2**, 1484.
7. D. C. Craig, D. S. Reddy and G. R. Desiraju, *J. Am. Chem. Soc.*, 1996, **118**, 4090.
8. R. Pepinsky, *Phys. Rev.*, 1955, **100**, 971.
9. G. M. Schmidt, *Pure Appl. Chem*, 1971, **27**, 647.

10. K. K. Arora, T. R. Shattock, P. Vishweshwar and M. Zaworotko, *Cryst. Growth Des.*, 2008, **8**, 4533.
11. G. R. Desiraju, *Crystal Engineering, The design of Organic Solids*, Elsevier:Amsterdam, 1989.
12. M. W. Hosseini, *Acc. Chem. Res.*, 2005, **38**, 313.
13. J. K. Swearingen, L. Brammer, E. A. Bruton and P. Sherwood, *PNAS*, 2002, **99**, 4956.
14. A. M. Beatty, B. A. Helfrich and C. B. Aakeroy, *Angew. Chem. Int. Ed.*, 2001, **40**, 3240.
15. E. J. Corey, *Chem. Soc. Rev.*, 1988, **17**, 111.
16. V. A. Russel and M. D. Ward, *Chem. Mater.*, 1996, **8**, 1654.
17. J. D. Dunitz and J. Bernstein, *Acc. Chem. Res.*, 1995, **28**, 193.
18. G. R. Desiraju, *J. Mol. Struct.*, 2003, **656**, 5.
19. R. Taylor and O. Kennard, *Acc. Chem. Res.*, 1984, **17**, 320.
20. W. M. Latimer and W. H. Rodebush, *J. Am. Chem. Soc.*, 1920, **42**, 1419.
21. G. C. Pimentel and A. L. McClellan, *The Hydrogen Bond*, Freeman San Francisco, 1960.
22. T. Steiner, *Angew. Chem. Int. Ed.*, 2002, **41**, 48.
23. G. R. Desiraju, *The Weak Hydrogen Bond in Structural and Chemical Biology*, Oxford University Press, Oxford, 1999.
24. S. L. James, *Chem. Soc. Rev.*, 2003, **32**, 276.
25. G. M. Whitesides and M. Bonchevea, *PNAS*, 2002, **99**, 4769.
26. J. A. Palesko, *Self Assembly: The science of things that put themselves together*, Chapman & Hall, 2007.
27. M. A. West, Y. L. Chang, F. W. Fowler and J. W. Lauher, *J. Am. Chem. Soc.*, 1993, **115**, 5991.
28. C. Janiak, *Dalton Trans.*, 2003, 2781.
29. D. J. Kleinhans, L. Dobrzanska and L. J. Barbour, *New J. Chem.*, 2008, **32**.
30. G. O. Lloyd, L. Dobrzanska and L. J. Barbour, *New J. Chem.*, 2007, **31**, 669.
31. J. Vondrasek and L. Rulisek, *J. Inorg. Biochem.*, 1998, **71**, 115.
32. T. A. Okamura, G. C. Xu, Y. Q. Huang, G. X. Liu, W. Y. Sun and N. Ueyama, *CrystEngComm*, 2008, **10**, 1052.
33. R. Villar, P. Diaz, and A. J. P. White, *Inorg. Chem.*, 2006, **45**, 1617.
34. M. O'Keeffe, O. M. Yaghi, N. W. Ockwig, H. K. Chae, M. Eddaoudi and J. Kim, *Nature*, 2003, **423**, 705.
35. R. Stuart and R. Robson, *Angew. Chem. Int. Ed.*, 1998, **37**, 1460.

36. B. Liu and L. Xu, *Inorg. Chem. Commun.*, 2006, **9**, 364.
37. S. Subramanian, M. J. Zaworotko and S. B. Copp, *J. Am. Chem. Soc.*, 1992, **114**, 8719
38. S. Sabramanian and M. J. Zaworotko, *Angew. Chem. Int. Ed.*, 1995, **34**, 2127.
39. O. M. Yaghi and H. Li, *Angew. Chem. Int. Ed. Engl.*, 1995, **34**, 207.
40. E. Matwey, C. L. Schauer, F. W. Fowler, and J. W. Lauher, *J. Am. Chem. Soc.*, 1997, **119**, 10245.
41. J. J. Kane, S. Coe, T. L. Nguyen, L. M. Toledo, E. Wininger, J. W. Lauher and F. W. Fowler, *J. Am. Chem. Soc.*, 1997, **119**, 86.
42. Y. Kumamoto, S. Kitagawa and K. Uemura, *Chem. Eur. J.*, 2008, **14**, 9565.
43. Y. Huang, B. Tzeng, B. Chen, W. Wu, S. Lee, S. Peng and G. Lee, *Inorg. Chem.*, 2007, **46**, 186.
44. M. Li, Q. Zeng, D. Wu, S. Lei, C. Liu, L. Piao, S. An, Y. Yang and C. Wang, *Cryst. Growth. Des.*, 2008, **8**, 869.
45. G. W. Orr, J. L. Atwood and L. J. Barbour, *Nature*, 1998, **393**, 671.
46. L. J. Barbour, J. L. Atwood and G. O. Lloyd, *Chem. Commun.*, 2005, 1845.
47. B. De Silva, M. J. Plater, J. P. Sinclair, T. Gelbrich and M. B. Hursthouse, *J. Mol. Struct.*, 2006, **784**, 269.
48. J. L. Atwood, G. W. Orr and L. J. Barbour, *Chem. Commun.*, 2000, 859.
49. W. Y. Sun, T. Okamura, Y. Wang and N. Ueyama, *Cryst. Growth. Des.*, 2008, **8**, 802.
50. R. Matsuda, S. Horike, S. Hasegawa, S. Furukawa, Y. Kinoshita, K. Mochizuki and S. Kitagawa, *J. Am. Chem. Soc.* 2007, **129**, 2607
51. R. J. Saykally, J. D. Cruzan and K. Liu, *Science*, 1996, **271**, 929.
52. A. Liljas, *Nature New Biology*, 1972, **235**, 131.
53. E.N Baker, *J. Mol. Biol.*, 1980, **141**, 441.
54. H-L. Hu, Y-F. Hsu, C-J. Wu, C-W. Yeh, D. M. Proserpio and J-D. Chen, *CrystEngComm*, 2009, **11**, 168.

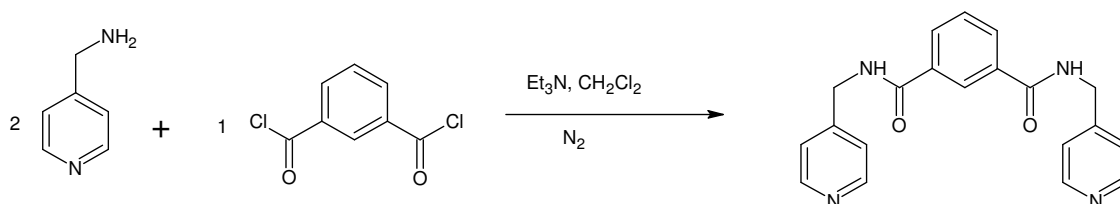
Chapter 2

Experimental

This chapter describes the synthesis and characterization of the ligands as well as their crystallizations with a variety of different metal salts. The instrumentation and computer programmes used for the study are also described.

2.1 Synthesis and characterization of ligands

2.1.1 Preparation of *N,N'*-bis(pyridin-4-ylmethyl)isophthalamide (ISO)^{1,2}

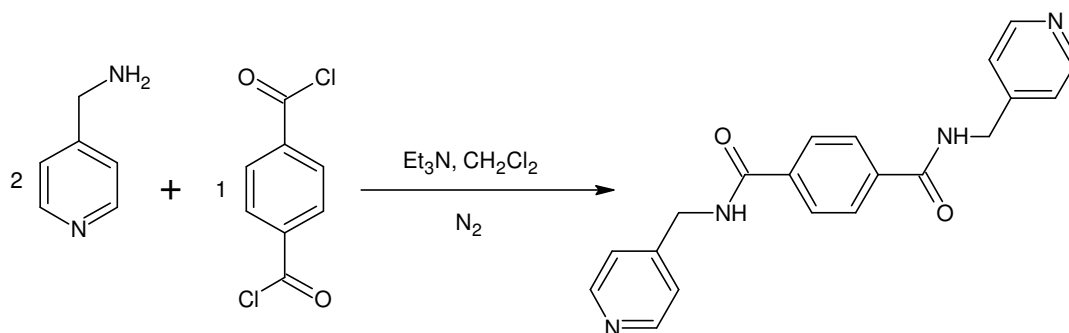


Scheme 2.1. Synthesis of *N,N'*-bis(pyridin-4-ylmethyl)isophthalamide.

Triethylamine (2.97 g, 29.4 mmol) and 4-(aminomethyl)pyridine (3.21 g, 29.4 mmol) were mixed together in a quick-fit three-necked round bottomed flask. A solution of isophthaloyl chloride (3.0 g, 14.7 mmol) in dichloromethane 30 mL was added over 30 minutes at 0° C under nitrogen. The reaction was stirred for 8 hours and the resulting orange precipitate was filtered off and dried in a desiccator for 24 hours. The crude product was mixed with 40 mL water, followed by filtration, to yield a white powder.

Yield 85%. ¹H-NMR (DMSO-d₆, 400MHz): δ 4.49 (2H, d, *J* = 6.2, Py-CH₂), δ 7.30 (2H, d, *J* = 5.9, Py-H), δ 7.60 (1H, t, *J* = 8.8, 7.9, Ar-H), δ 8.06 (1H, dd, *J* = 1.47, 2.05, Ar-H), δ 8.45 (1H, s, Ar-H), δ 8.49 (2H, d, *J* = 5.0, Py-H), δ 9.26 (1H, t, *J* = 5.6, 6.8, N-H). FTIR-ATR: ν_{\max} : 3491 cm⁻¹ (N-H stretch) 3068 cm⁻¹ (≡C-H stretch) 1605 cm⁻¹ 1478 cm⁻¹ (C≡C stretch), 716 cm⁻¹, 696 cm⁻¹ (≡C-H out-of-plane (oop) bend), 1564 cm⁻¹ (N-H bend), 1478 cm⁻¹ (CH₂ bend). MS (ESI+): *m/z* 347 (55% ([M+H]⁺)), 174 (100%), 102 (98%).

2.1.2 Preparation of *N,N'*-bis(pyridin-4-ylmethyl)terephthalamide (TER)¹

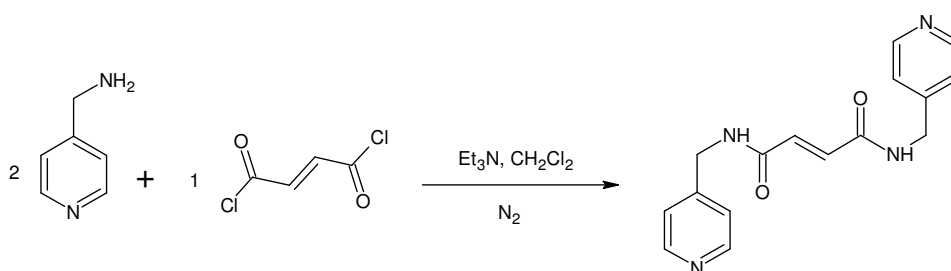


Scheme 2.2. Synthesis of *N,N'*-bis(pyridin-4-ylmethyl)terephthalamide.

The same procedure as above was used for the synthesis of **TER**, except that terephthaloyl chloride was used instead of isophthaloyl chloride. The product was obtained as a white powder.

Yield 75%. ¹H-NMR (DMSO-d₆, 400MHz): δ 4.51 (2H, d, *J* = 5.9, Py-CH₂), δ 7.31 (2H, d, *J* = 5.9, Py-*H*), δ 8.0 (1H, s, Ar-*H*), δ 8.50 (2H, d, *J* = 6.2, Py-*H*), δ 9.30 (1H, t, *J* = 5.9, 6.2, N-*H*). FTIR-ATR: ν_{\max} 3455 cm⁻¹ (N-H stretch) 3010 cm⁻¹, (≡C-H stretch), 1638 cm⁻¹ (C=O stretch), 1607 cm⁻¹, 1455 cm⁻¹ (C≡C stretch), 1552 cm⁻¹, 1562 cm⁻¹ (N-H bend), 1455 cm⁻¹ (CH₂ bend). MS (ESI+): *m/z* 347 (98% ([M+H]⁺)), 174 (100%), 102 (73%).

2.1.3 Preparation of (2*E*)-*N,N'*-bis(2-pyridin-4-ylethyl)but-2-enediamide (FUM)¹



Scheme 2.3. Synthesis of (2*E*)-*N,N'*-bis(2-pyridin-4-ylethyl)but-2-enediamide.

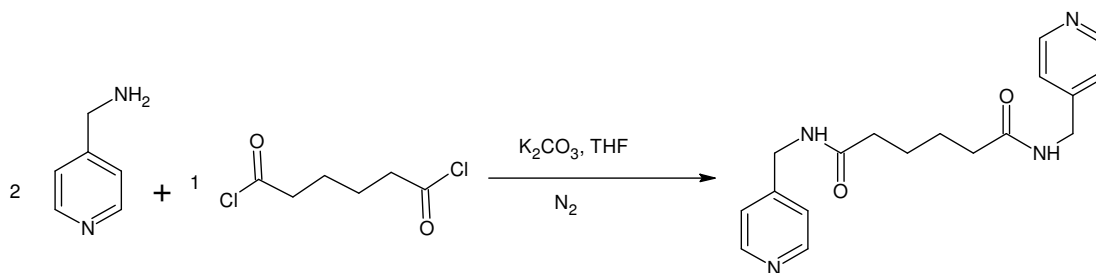
4-(Aminomethyl)pyridine (2.83 g, 26 mmol) and triethylamine (3.62 g, 26 mmol) were cooled to 0° C under nitrogen. A solution of fumaroyl chloride (2 g, 13 mmol) in THF (30 mL) was added slowly over a 30 minute period. The reaction mixture was allowed to warm to room temperature and refluxed for two days. The precipitate was filtered off, washed with THF and dried in a desiccator for 24 hours. The crude product was washed with saturated NaOH and recrystallized from ethanol.

Yield 60%. $^1\text{H-NMR}$ (DMSO- d_6 , 400MHz): δ 4.40 (2H, d, $J = 6.7$, Py- CH_2), δ 4.4 (1H, s, =C- H), δ 7.3 (2H, d, $J = 5.3$, Py- H), δ 8.50 (2H, d, $J = 7.8$, Py- H), δ 9.0 (1H, s, N- H). FTIR-ATR: ν_{max} : 3426 cm^{-1} (N- H stretch), 3076 cm^{-1} , 3184 cm^{-1} , 3266 cm^{-1} C- H aromatic and alkene), 1629 cm^{-1} (C=O stretch), 1606 cm^{-1} (C \equiv C stretch alkene), 1563 cm^{-1} , 1447 cm^{-1} (C \equiv C aromatic), 1497 cm^{-1} (CH_2 bend). MS (ESI+): m/z 297 (97%, ($[\text{M}+\text{H}]^+$)), 149 (100%), 102 (28%).

2.1.4 Preparation of N,N' -bis(pyridin-4-ylmethyl)succinamide SUC

The ligand SUC used in this study was provided by Professor L. J. Barbour.

2.1.5 Preparation of N,N' -bis(pyridin-4-ylmethyl)hexanediamide (ADI)³

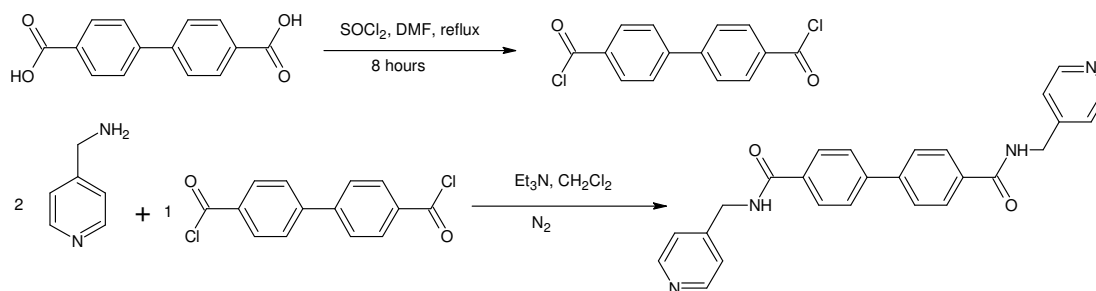


Scheme 2.4. Synthesis of N,N' -bis(pyridin-4-ylmethyl)hexanediamide.

4-(aminomethyl)pyridine (1 g, 9.25 mmol) and anhydrous potassium carbonate (11.067 g, 80 mmol) were dissolved in dry THF (7 mL). Adipoyl chloride (1.35 mL, 4.625 mmol) in THF (7 mL) was added to the solution and stirred under nitrogen atmosphere at 0°C overnight. The solvent was evaporated and residue was washed with water and methylene chloride. The product was purified by recrystallization from ethanol to yield colourless crystals.

Yield 70%. $^1\text{H-NMR}$ (DMSO- d_6 , 400MHz): δ 1.58 (2H, m, O=C CH_2CH_2), δ 2.20 (2H, m, O=C H_2CH_2), δ 4.29 (2H, d, $J = 7.6$, Py- CH_2), δ 7.23 (2H, d, $J = 5.9$, Py- H), δ 8.42 (1H, t, $J = 5.3, 8.5$, N- H), δ 8.48 (1H, d, $J = 6.2$, Py- H). FTIR-ATR: ν_{max} : 3277 cm^{-1} (N- H stretch), 3105 cm^{-1} (-C \equiv CH stretch), 1636 cm^{-1} (C=O stretch), 1606 cm^{-1} , 1454 cm^{-1} (C \equiv C stretch), 1556 cm^{-1} (N- H bend), 1454 cm^{-1} (CH_2 bend). MS (ESI+): m/z (95% ($[\text{M}+\text{H}]^+$)), 164 (100%), 102 (83%).

2.1.6 Preparation of *N,N'*-bis(pyridin-4-ylmethyl)biphenyl-4,4'-dicarbonyl dicarboxamide (DIP)¹

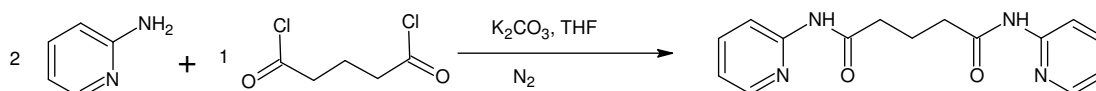


Scheme 2.5. Synthesis of *N,N'*-bis(pyridin-4-ylmethyl)biphenyl-4,4'-dicarbonyl dicarboxamide.

10 g of (1,1-biphenyl)-4,4'-dicarboxylic acid was converted to (1,1-biphenyl)-4,4'-dicarbonyl chloride by reaction with excess thionyl chloride. A solution of (1,1-biphenyl)-4,4'-dicarbonyl chloride, (4.01 g, 14.7 mmol) in 50 mL dichloromethane was added slowly, over a 30 minute period, to a mixture of 4-(aminomethyl)pyridine (29.4 mmol, 3.21 g) and triethylamine (29.4 mmol, 2.97 g). The mixture was allowed to stir overnight under a nitrogen atmosphere at 0° C. The resulting orange precipitate was filtered off and dried in a desiccator for 24 hours. The crude product was mixed with saturated NaOH and mixed with 40 mL water followed by filtration and recrystallization from ethanol.

Yield 79%. ¹H-NMR (DMSO-d₆, 400MHz): δ 4.53 (2H, d, *J* = 5.9 Py-CH₂), δ 7.32 (2H, d, *J* = 8.51 Py-H), δ 7.87 (2H, d, *J* = 6.2, Ar-H), δ 8.03 (2H, d, *J* = 4.1, Ar-H), δ 8.51 (2H, d, *J* = 5.6 Py-H), δ 9.22 (1H, t, *J* = 6.4, 6.2, N-H). FTIR-ATR: ν_{max} 3234 cm⁻¹ (N-H stretch), 3070 cm⁻¹ (≡C-H stretch), 1606 cm⁻¹ (C=O stretch), 1550 cm⁻¹ (N-H bend), 1491 cm⁻¹ (C≡C stretch), 1412 cm⁻¹ (CH₂ bend). MS (ESI⁺): *m/z* 423 (85%, ([M+H]⁺)), 212 (100%), 106 (10%).

2.1.8 Preparation of *N,N'*-dipyridin-2-ylpentanediamide (GLUT)³



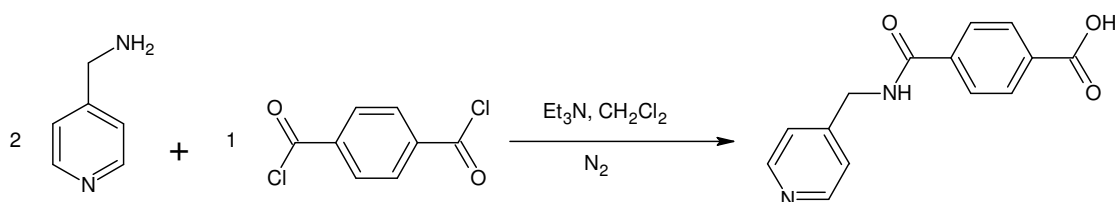
Scheme 2.6. Synthesis of *N,N'*-dipyridin-2-ylpentanediamide.

2-Aminopyridine (5.97 g, 63.5 mmol) and potassium carbonate (11.067 g, 80 mmol) were dissolved in THF (41 mL) and glutaryl chloride (3.972 g, 24 mmol) was then added. The mixture was stirred at 0° C, under nitrogen for 12 hours. The solvent was evaporated and the

residue was suspended in water after which it was extracted with methylene chloride and recrystallized from ethanol to yield colourless block shaped crystals.

Yield 60%. $^1\text{H-NMR}$ (DMSO- d_6 , 400MHz): δ 1.87 (2H, m, $\text{O}=\text{CCH}_2\text{CH}_2$), δ 2.42 (2H, t, $J = 7.6$, $\text{O}=\text{CCH}_2\text{CH}_2$), δ 7.05 (1H, t, $J = 6.2$, Py- H), δ 7.73 (1H, t, $J = 8.2$, Py- H), δ 8.07 (1H, d, $J = 8.2$, Py- H), δ 8.27 (1H, t, $J = 4.3$, Py- H), δ 10.41 (s, 1H, N- H). FTIR-ATR: ν_{max} 3180 cm^{-1} (N- H stretch), 3117 cm^{-1} ($-\text{C}\equiv\text{CH}$ stretch), 2961 cm^{-1} ($-\text{C}-\text{H}$ stretch), 1692 cm^{-1} ($\text{C}=\text{O}$ stretch), 1577 cm^{-1} (N- H bend), 1467 cm^{-1} (aromatic $\text{C}\equiv\text{C}$ stretch) 1456 cm^{-1} (CH_2 bend). MS (ESI+) m/z 285 (98% ($[\text{M}+\text{H}]^+$)), 143 (100%).

2.1.9 Preparation of 4-(pyridin-4-ylmethyl)aminocarbonyl benzoic acid (TER-A)¹



Scheme 2.7. Synthesis of 4-(pyridin-4-ylmethyl)aminocarbonyl benzoic acid.

Ligand **TER-A** was synthesized serendipitously from a reaction that was intended to make **TER**. It is believed that **TER-A** is a product of the incomplete reaction between terephthaloyl chloride and 4-(aminomethyl)pyridine.

2.2 Crystallizations of the ligands with metal salts

The fully characterised ligands were crystallized with various metal salts. These ligands were found to dissolve in alcohols, water, dimethylformamide (DMF) and dimethylsulphoxide (DMSO). Crystallizations were first carried out using the solvent evaporation method. The layering and solvothermal methods were only employed for crystallizations of ligands **DIP** and **TER-A**, which did not yield any crystals with the solvent evaporation method.

2.2.1 Solvent evaporation method

Crystallizations were set up in ethanol, methanol and DMF using metal to ligand ratios of 1:1, 1:2, 2:1 and 4:1. For a typical crystallization experiment, the ligand and the metal salt were dissolved separately in a minimum amount of solvent, mixed together in a 10 mL vial, followed by slow evaporation of the solvent. Crystallizations in ethanol/methanol alone yielded precipitates after a few minutes whereas a mixture of ethanol and water or methanol

and water did not yield precipitates. In some cases, a precipitate formed after a few days, in such cases the precipitate was redissolved and solvent was then allowed to evaporate. The reaction conditions of all crystallizations set up, as well as the nature of the product obtained in each case is given in Tables 2.2-2.10. Table 2.1 below explains the symbols used in these tables.

Table 2.1. Explanation of symbols used in Tables 2.2-2.10 to describe types of products obtained

Symbol	Description
1-17	Single crystals were obtained
a	Polycrystalline material was obtained
b	Single crystals with unit cell corresponding to that of the free ligand
c	Single crystals with unit cell corresponding to that of the metal salt
d	Single crystals too small or not suitable for SCD analysis experiment
e	An oily substance was obtained

2.2.2 Solvothermal method

This method was only carried out with either **DIP** or **TER** with nitrates of zinc, copper, nickel and cobalt in a metal to ligand ratio of 1:1. The ligand and the metal salt were dissolved in DMF. The solution was stirred for 10 minutes at room temperature and placed in a hydrothermal pressure vessel. The mixture was heated at 110° C for three days.

2.2.3 Layering method

A solution of the metal salt in ethanol (1 mL) was carefully layered upon a solution of the ligand in DMSO (1 mL). A buffer consisting of a DMSO/ethanol mixture was placed between the two layers.

Crystallizations of FUM with a variety of metal salts

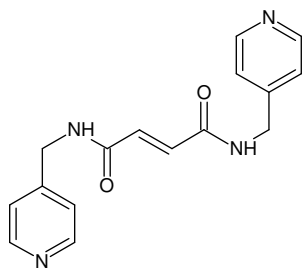


Table 2.2. Crystallizations of **FUM** with a variety of metal salts

Metal salt	MeOH, M:L ratio	EtOH, M:L ratio	DMF, M:L ratio
Cd(NO ₃) ₂ ·4H ₂ O	1:1 1:2 2:1 4:1 a a a a	1:1 1:2 2:1 4:1 a a a a	1:1 1:2 2:1 4:1 a a a a
Zn(NO ₃) ₂ ·4H ₂ O	1:1 1:2 2:1 4:1 a a a a	1:1 1:2 2:1 4:1 a a a a	1:1 1:2 2:1 4:1 a a a a
Cu(NO ₃) ₂ ·4H ₂ O	1:1 1:2 2:1 4:1 a a a a	1:1 1:2 2:1 4:1 a a a 2	1:1 1:2 2:1 4:1 a a a a
CuCl ₂ ·4H ₂ O	1:1 1:2 2:1 4:1 a a a a	1:1 1:2 2:1 4:1 a a a a	1:1 1:2 2:1 4:1 a a a a
CuSO ₄ ·5H ₂ O	1:1 1:2 2:1 4:1 a a a a	1:1 1:2 2:1 4:1 a a a 1	1:1 1:2 2:1 4:1 a a a a
CoCl ₂ ·H ₂ O	1:1 1:2 2:1 4:1 a a a 4	1:1 1:2 2:1 4:1 a a a a	1:1 1:2 2:1 4:1 a a d 4
Cu(BF ₄) ₂ ·xH ₂ O	1:1 1:2 2:1 4:1 a a a a	1:1 1:2 2:1 4:1 a a a a	1:1 1:2 2:1 4:1 a a a a
Mn(NO ₃) ₂ ·H ₂ O	1:1 1:2 2:1 4:1 a a a b	1:1 1:2 2:1 4:1 b b b b	1:1 1:2 2:1 4:1 a a a a
MnCl ₂ ·4H ₂ O	1:1 1:2 2:1 4:1 a a a a	1:1 1:2 2:1 4:1 a a a a	1:1 1:2 2:1 4:1 a a a a
MnBr ₂ ·4H ₂ O	1:1 1:2 2:1 4:1 a a a a	1:1 1:2 2:1 4:1 a a a a	1:1 1:2 2:1 4:1 a a a a
Ni(NO ₃) ₂ ·6H ₂ O	1:1 1:2 2:1 4:1 a a a a	1:1 1:2 2:1 4:1 a a a a	1:1 1:2 2:1 4:1 a a a a
NiBr ₂ ·6H ₂ O	1:1 1:2 2:1 4:1 a a a a	1:1 1:2 2:1 4:1 a a a a	1:1 1:2 2:1 4:1 a a a a
NiCl ₂ ·6H ₂ O	1:1 1:2 2:1 4:1 a a a a	1:1 1:2 2:1 4:1 a a a 3	1:1 1:2 2:1 4:1 a a a c

Crystallizations of SUC with a variety of metal salts

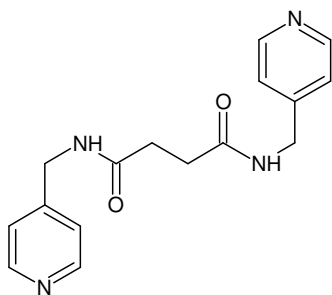


Table 2.3. Crystallizations of SUC with a variety of metal salts

Metal salt	EtOH, M:L ratio	DMF, M:L ratio
Cd(NO ₃) ₂ ·4H ₂ O	1:1 1:2 2:1 4:1 a a a a	1:1 1:2 2:1 4:1 a a a a
Zn(NO ₃) ₂ ·4H ₂ O	1:1 1:2 2:1 4:1 a a a a	1:1 1:2 2:1 4:1 a a a a
Cu(NO ₃) ₂ ·4H ₂ O	1:1 1:2 2:1 4:1 a a a a	1:1 1:2 2:1 4:1 a a a a
CuCl ₂ ·4H ₂ O	1:1 1:2 2:1 4:1 a a a a	1:1 1:2 2:1 4:1 a a a a
CuSO ₄ ·5H ₂ O	1:1 1:2 2:1 4:1 a a a a	1:1 1:2 2:1 4:1 a a a a
NiBr ₂ ·6H ₂ O	1:1 1:2 2:1 4:1 a a a a	1:1 1:2 2:1 4:1 a a a a
Co(NO ₃) ₂ ·4H ₂ O	1:1 1:2 2:1 4:1 a a a a	1:1 1:2 2:1 4:1 a a a a
NiCl ₂ ·6H ₂ O	1:1 1:2 2:1 4:1 a a a a	1:1 1:2 2:1 4:1 a a a a
Ni(NO ₃) ₂ ·6H ₂ O	1:1 1:2 2:1 4:1 a a a a	1:1 1:2 2:1 4:1 a a a a
CoCl ₂ ·H ₂ O	1:1 1:2 2:1 4:1 a a a 5	1:1 1:2 2:1 4:1 a a a a

Crystallizations of **ADI** with a variety of metal salts

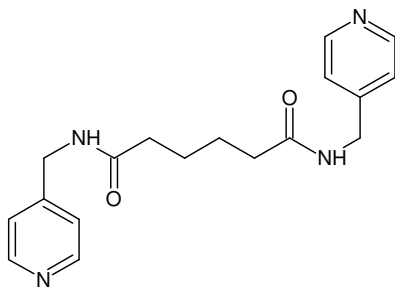


Table 2.4. Crystallizations of **ADI** with a variety of metal salts

Metal salt	MeOH, M:L ratio	EtOH, M:L ratio	DMF, M:L ratio
Cd(NO ₃) ₂ ·4H ₂ O	1:1 1:2 2:1 4:1 6 a a a	1:1 1:2 2:1 4:1 6 9 a a	1:1 1:2 2:1 4:1 a a a a
Zn(NO ₃) ₂ ·4H ₂ O	1:1 1:2 2:1 4:1 a a a a	1:1 1:2 2:1 4:1 a 7 8 a	1:1 1:2 2:1 4:1 a 7 a a
Cu(NO ₃) ₂ ·4H ₂ O	1:1 1:2 2:1 4:1 a a a a	1:1 1:2 2:1 4:1 10 10 10 a	1:1 1:2 2:1 4:1 d d 10 c
CuCl ₂ ·4H ₂ O	1:1 1:2 2:1 4:1 a a a a	1:1 1:2 2:1 4:1 a a a a	1:1 1:2 2:1 4:1 ? a a a
CuSO ₄ ·5H ₂ O	1:1 1:2 2:1 4:1 a a a a	1:1 1:2 2:1 4:1 a a a a	1:1 1:2 2:1 4:1 c c c c
CoCl ₂ ·H ₂ O	1:1 1:2 2:1 4:1 a a a a	1:1 1:2 2:1 4:1 a a a 11	1:1 1:2 2:1 4:1 c c c c
Cu(BF ₄) ₂ ·xH ₂ O	1:1 1:2 2:1 4:1 a a a a	1:1 1:2 2:1 4:1 a a a a	1:1 1:2 2:1 4:1 a a a a
Mn(NO ₃) ₂ ·H ₂ O	1:1 1:2 2:1 4:1 a a a a	1:1 1:2 2:1 4:1 a a a a	1:1 1:2 2:1 4:1 a a a a
MnCl ₂ ·4H ₂ O	1:1 1:2 2:1 4:1 a a a a	1:1 1:2 2:1 4:1 a a a a	1:1 1:2 2:1 4:1 a a a a
MnBr ₂ ·4H ₂ O	1:1 1:2 2:1 4:1 a d a d	1:1 1:2 2:1 4:1 d d d 12	1:1 1:2 2:1 4:1 c c c c
Ni(NO ₃) ₂ ·6H ₂ O	1:1 1:2 2:1 4:1 a a a a	1:1 1:2 2:1 4:1 a a a a	1:1 1:2 2:1 4:1 a a a a
NiBr ₂ ·6H ₂ O	1:1 1:2 2:1 4:1 a a a a	1:1 1:2 2:1 4:1 a a a a	1:1 1:2 2:1 4:1 a c c c
NiCl ₂ ·6H ₂ O	1:1 1:2 2:1 4:1 a a a a	1:1 1:2 2:1 4:1 a a a a	1:1 1:2 2:1 4:1 a a a a

Crystallizations of **GLUT** with a variety of metal salts

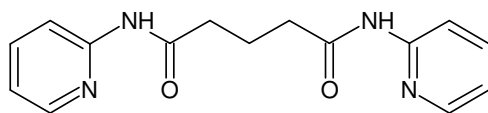


Table 2.5. Crystallizations of **GLUT** with a variety of metal salts

Metal salt	MeOH, M:L ratio	EtOH, M:L ratio	DMF, M:L ratio
Cd(NO ₃) ₂ ·4H ₂ O	1:1 1:2 2:1 4:1 b b b 14	1:1 1:2 2:1 4:1 b b b 14	1:1 1:2 2:1 4:1 a a a a
Zn(NO ₃) ₂ ·4H ₂ O	1:1 1:2 2:1 4:1 b b b 15	1:1 1:2 2:1 4:1 b b b 15	1:1 1:2 2:1 4:1 a a a a
Cu(NO ₃) ₂ ·4H ₂ O	1:1 1:2 2:1 4:1 a a a a	1:1 1:2 2:1 4:1 a a a a	1:1 1:2 2:1 4:1 a a a a
CuCl ₂ ·4H ₂ O	1:1 1:2 2:1 4:1 a a a a	1:1 1:2 2:1 4:1 a a a a	1:1 1:2 2:1 4:1 a a a a
CuSO ₄ ·5H ₂ O	1:1 1:2 2:1 4:1 a a a a	1:1 1:2 2:1 4:1 a a a a	1:1 1:2 2:1 4:1 a a a a
Co(NO ₃) ₂ ·4H ₂ O	1:1 1:2 2:1 4:1 b a a a	1:1 1:2 2:1 4:1 a a a a	1:1 1:2 2:1 4:1 a a a a
NiCl ₂ ·6H ₂ O	1:1 1:2 2:1 4:1 a a a a	1:1 1:2 2:1 4:1 a a a a	1:1 1:2 2:1 4:1 a a a a
Ni(NO ₃) ₂ ·6H ₂ O	1:1 1:2 2:1 4:1 a a a a	1:1 1:2 2:1 4:1 a a a a	1:1 1:2 2:1 4:1 a a a a
CoCl ₂ ·H ₂ O	1:1 1:2 2:1 4:1 a a a a	1:1 1:2 2:1 4:1 a a a a	1:1 1:2 2:1 4:1 a a a a

Crystallizations of ISO with a variety of metal salts

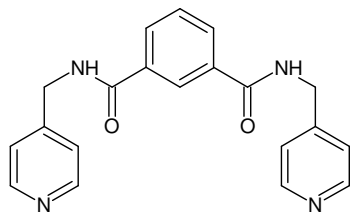


Table 2.6. Crystallizations of ISO with a variety of metal salts

Metal salt	MeOH, M:L ratio	EtOH, M:L ratio	DMF, M:L ratio
Cd(NO ₃) ₂ ·4H ₂ O	1:1 1:2 2:1 4:1 d d d d	1:1 1:2 2:1 4:1 a d a d	1:1 1:2 2:1 4:1 a a a a
Zn(NO ₃) ₂ ·4H ₂ O	1:1 1:2 2:1 4:1 16 16 d a	1:1 1:2 2:1 4:1 16 16 a a	1:1 1:2 2:1 4:1 a a a a
CuCl ₂ ·4H ₂ O	1:1 1:2 2:1 4:1 a a a a	1:1 1:2 2:1 4:1 a a a a	1:1 1:2 2:1 4:1 e e e e
CuSO ₄ ·5H ₂ O	1:1 1:2 2:1 4:1 a c c c	1:1 1:2 2:1 4:1 a a a a	1:1 1:2 2:1 4:1 c c c c
Co(Cl) ₂ ·4H ₂ O	1:1 1:2 2:1 4:1 a a a a	1:1 1:2 2:1 4:1 a a a a	1:1 1:2 2:1 4:1 a a a a
Ni(NO ₃) ₂ ·6H ₂ O	1:1 1:2 2:1 4:1 a a a a	1:1 1:2 2:1 4:1 a a a a	1:1 1:2 2:1 4:1 a a a a
NiCl ₂ ·6H ₂ O	1:1 1:2 2:1 4:1 a a a a	1:1 1:2 2:1 4:1 a a a a	1:1 1:2 2:1 4:1 a a a a
MnBr ₂ ·4H ₂ O	1:1 1:2 2:1 4:1 a a a a	1:1 1:2 2:1 4:1 a a a a	1:1 1:2 2:1 4:1 a a a a
MnCl ₂ ·4H ₂ O	1:1 1:2 2:1 4:1 a a a a	1:1 1:2 2:1 4:1 a a a a	1:1 1:2 2:1 4:1 a a a a
Mn(NO ₃) ₂ ·H ₂ O	1:1 1:2 2:1 4:1 a a a a	1:1 1:2 2:1 4:1 a a a a	1:1 1:2 2:1 4:1 a a a a
Cu(BF ₄) ₂ ·xH ₂ O	1:1 1:2 2:1 4:1 a a a a	1:1 1:2 2:1 4:1 a a a a	1:1 1:2 2:1 4:1 a a a a

Crystallizations of **TER** with a variety of metal salts

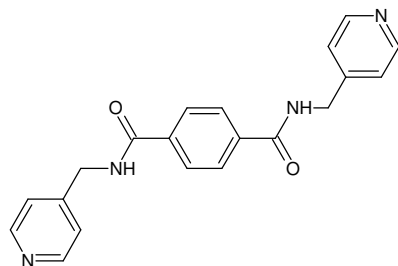


Table 2.7. Crystallizations of **TER** with a variety of metal salts

Metal salt	EtOH, M:L ratio				DMF, M:L ratio			
Cd(NO ₃) ₂ ·4H ₂ O	1:1	1:2	2:1	4:1	1:1	1:2	2:1	4:1
	d	d	d	d	b	b	b	b
Zn(NO ₃) ₂ ·4H ₂ O	1:1	1:2	2:1	4:1	1:1	1:2	2:1	4:1
	a	a	a	a	b	b	b	a
CuCl ₂ ·4H ₂ O	1:1	1:2	2:1	4:1	1:1	1:2	2:1	4:1
	a	a	a	a	a	a	a	a
CuSO ₄ ·5H ₂ O	1:1	1:2	2:1	4:1	1:1	1:2	2:1	4:1
	a	a	a	a	a	a	a	a
Co(Cl) ₂ ·4H ₂ O	1:1	1:2	2:1	4:1	1:1	1:2	2:1	4:1
	a	a	a	a	a	a	a	a
Ni(NO ₃) ₂ ·6H ₂ O	1:1	1:2	2:1	4:1	1:1	1:2	2:1	4:1
	a	a	a	a	b	b	b	b
NiCl ₂ ·6H ₂ O	1:1	1:2	2:1	4:1	1:1	1:2	2:1	4:1
	a	a	a	a	a	a	a	a
MnBr ₂ ·4H ₂ O	1:1	1:2	2:1	4:1	1:1	1:2	2:1	4:1
	a	a	a	a	a	a	a	a
MnCl ₂ ·4H ₂ O	1:1	1:2	2:1	4:1	1:1	1:2	2:1	4:1
	a	a	a	a	a	a	a	a
Mn(NO ₃) ₂ ·6H ₂ O	1:1	1:2	2:1	4:1	1:1	1:2	2:1	4:1
	a	a	a	a	b	b	b	b
Cu(NO ₃) ₂ ·4H ₂ O	1:1	1:2	2:1	4:1	1:1	1:2	2:1	4:1
	a	a	a	a	a	a	a	a

Crystallizations of TER-A with a variety of metal salts

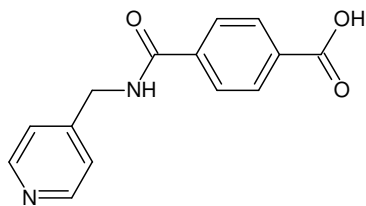


Table 2.8. Crystallizations of TER-A with a variety of metal salts

Metal salt	EtOH, M:L ratio				DMF, M:L ratio			
Cu(NO ₃) ₂ ·4H ₂ O	1:1	1:2	2:1	4:1	1:1	1:2	2:1	4:1
	a	a	a	a	d	a	a	a
Mn(NO ₃) ₂ ·H ₂ O	1:1	1:2	2:1	4:1	1:1	1:2	2:1	4:1
	a	a	a	b	a	c	a	b
Ni(NO ₃) ₂ ·6H ₂ O	1:1	1:2	2:1	4:1	1:1	1:2	2:1	4:1
	a	a	a	a	a	a	a	a
Cd(NO ₃) ₂ ·4H ₂ O	1:1	1:2	2:1	4:1	1:1	1:2	2:1	4:1
	a	a	a	a	a	a	a	a
Zn(NO ₃) ₂ ·4H ₂ O	1:1	1:2	2:1	4:1	1:1	1:2	2:1	4:1
	a	a	a	a	a	a	a	17

Crystallizations of DIP with a variety of metal salts

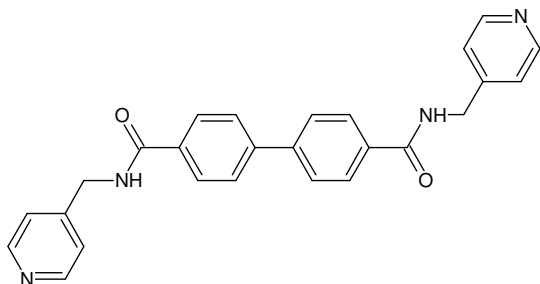


Table 2.9. Crystallizations of DIP with a variety of metal salts

Metal salt	EtOH, M:L ratio				DMF, M:L ratio			
Cd(NO ₃) ₂ ·4H ₂ O	1:1	1:2	2:1	4:1	1:1	1:2	2:1	4:1
	a	a	a	a	a	a	a	a
Zn(NO ₃) ₂ ·4H ₂ O	1:1	1:2	2:1	4:1	1:1	1:2	2:1	4:1
	a	a	c	a	a	a	a	b
CuCl ₂ ·4H ₂ O	1:1	1:2	2:1	4:1	1:1	1:2	2:1	4:1
	a	a	a	a	a	a	a	a
CuSO ₄ ·5H ₂ O	1:1	1:2	2:1	4:1	1:1	1:2	2:1	4:1
	a	a	a	a	a	a	a	a
Co(Cl) ₂ ·4H ₂ O	1:1	1:2	2:1	4:1	1:1	1:2	2:1	4:1
	a	a	a	a	a	a	a	a
Ni(NO ₃) ₂ ·6H ₂ O	1:1	1:2	2:1	4:1	1:1	1:2	2:1	4:1
	a	a	a	a	a	a	a	a
NiCl ₂ ·6H ₂ O	1:1	1:2	2:1	4:1	1:1	1:2	2:1	4:1
	a	a	a	a	a	a	a	a
MnBr ₂ ·4H ₂ O	1:1	1:2	2:1	4:1	1:1	1:2	2:1	4:1
	a	a	c	a	a	a	c	a
MnCl ₂ ·4H ₂ O	1:1	1:2	2:1	4:1	1:1	1:2	2:1	4:1
	a	a	a	a	a	a	a	a
Mn(NO ₃) ₂ ·H ₂ O	1:1	1:2	2:1	4:1	1:1	1:2	2:1	4:1
	a	a	a	a	a	a	a	a
Cu(NO ₃) ₂ ·4H ₂ O	1:1	1:2	2:1	4:1	1:1	1:2	2:1	4:1
	a	d	d	d	a	a	a	a

Co-crystallizations of trimesic acid (T) with the synthesized ligands (L)

Trimesic acid and the ligand in the specified ratio were ground together using a mortar and pestle. The resulting paste was dissolved in either DMF or H₂O. The solvent was then allowed to evaporate.

Table 2.10. Co-crystallizations of trimesic acid (T) with the synthesized ligands (L)

Ligand	DMF, T:L ratio			H ₂ O, T:L ratio		
TER	1:1 e	1:3 e	1:1.5 e	1:1 a	1:3 a	1:1.5 a
ISO	1:1 a	1:3 a	1:1.5 a	1:1 a	1:3 a	1:1.5 a
ADI	1:1 a	1:3 a	1:1.5 a	1:1 13	1:3 13	1:1.5 a
DIP	1:1 a	1:3 a	1:1.5 a	1:1 a	1:3 a	1:1.5 a
SUC	1:1 e	1:3 e	1:1.5 e	1:1 a	1:3 a	1:1.5 a
FUM	1:1 a	1:3 a	1:1.5 a	1:1 a	1:3 a	1:1.5 a
GLUT	1:1 a	1:3 a	1:1.5 a	1:1 a	1:3 a	1:1.5 a
TER A	1:1 e	1:3 e	1:1.5 e	1:1 a	1:3 a	1:1.5 a

2.3 Instrumentation and computer packages

2.3.1 Single crystal diffraction analysis (SCD)

Crystal quality was assessed by its ability to rotate plane polarized light, its transparency and its morphology. Crystals which were too large were cut to the desired size. Suitable crystals were mounted on a glass fibre using paratone oil. All intensity data were collected at 100 K on a Bruker SMART APEX CCD diffractometer⁴ with Mo fine focus sealed tube, a 0.5 mm Monocap collimator, and an Oxford Cryostream cooling system (700 Series Cryostream Plus). The data were collected using omega scans, and recorded using a CCD (charge coupled device) area detector with a detector to crystal distance of 60 mm. Data reduction and absorption corrections were carried out using the SAINT⁵ and SADABS⁶ programmes, respectively. The unit cell dimensions were refined on all data and space groups were assigned based on systematic absences and intensity statistics. The structures were solved by direct methods using SHELXS-97⁷ and refined by SHELXL-97 and the X-seed⁸ graphical user interface. All non-hydrogen atoms were refined anisotropically. Hydrogen atoms were placed on calculated positions where feasible or located in difference electron density maps. Images of all crystal structures were generated using the programme POV-Ray.⁹ Atomic labels and unit cell axis were inserted using POV-Label.

2.3.2 Powder X-ray Diffraction (PXRD)

Diffraction patterns were recorded on a PANalytical XPERT-PRO diffractometer system. Simulated powder patterns of crystal structures were calculated using the programme LAZY-Pulverix¹⁰ and compared with the experimental patterns to confirm that crystals selected were a representative of the bulk sample.

2.3.3 Nuclear Magnetic Resonance (NMR)

All samples were dissolved in deuterated dimethylsulphoxide (DMSO-d₆) and analysed using either a Varian Unity INOVA (400MHz) spectrometer or a Varian VNMRs (300MHz) spectrometer.

2.3.4 FTIR-ATR

All samples were analysed as neat solids on the Golden Gate ATR of a Nexus Thermo Nicolet 670 FTIR.

2.3.5 Liquid Chromatography Electrospray Ionisation Mass Spectrometry (LC ESI-MS)

All samples were analysed using a Waters API Quattro Micro spectrometer with the following settings: 3.5 kV capillary voltage, 15 V cone voltage, 100° C source temperature, 400° C desolvation temperature, desolvation gas flow rate 400 L/h and cone gas flow rate 50 L/h.

2.3.6 The Cambridge Structural Database (CSD)

The CSD¹¹ was used as a search tool for published data related to this work. The CSD records single crystal structures and powder diffraction results of compounds that have been determined by X-Ray diffraction and neutron diffraction studies and deposited as published or unpublished results.

2.4 References

1. M. J. Plater, S. Buchan, M. R. Foreman, B. M. De Silva, M. Z. Alexander and J. M. Slawin, *J. Chem. Cryst.* 2002, **32**, 5.
2. L. J. Barbour, J. L. Atwood and G. W. Orr. *Nature*, 1998, **393**, 671.
3. T. Tsugaru, N. Moriguchi and S. Amiya, *J. Mol. Struct.* 1999, **477**, 191.
4. *SAINT Data collection software, Version 6.45*; Madison, WI, Bruker AXS Inc. 2003.

5. *SMART Data Collection Software, Version 5.629*; Madison, WI, Bruker AXS Inc. 2003.
6. *SADBAS, Version 2.05*; Madison, WI, Bruker AXS Inc. 2002.
7. G. M Sheldrick. *Acta Crystallogr. Sect. A, Found. Crystallogr.*, 2008, **64**, 112
8. L. J. Barbour, *J. Supramol. Chem.*, 2001, **1**, 189.
9. POV-RayTM, Version 3.6. Williamstone, Persistence of Vision Raytracer Pty. Ltd., 2004.
10. K. Yvon, W. Jeitschko and E. Parthe, *J. Appl. Crystallogr.*, 1997, **10**, 73.
11. F. Allen, *Acta Crystallogr., Sect. B*, 2002, **58**, 380.

Chapter 3

Crystal Structure Descriptions of the Pure Ligands

3.1 Introduction

This chapter describes crystal structures of the following ligands: **TER**, **ADI**, **DIP**, **GLUT** and **TER-A**. A crystal structure of **FUM** has been reported¹ and a crystal structure of **ISO** could not be obtained because all crystallization experiments yielded either a powder or crystals that were not suitable for single crystal diffraction (SCD) analysis. The crystallographic data and details of the structure solution and refinement procedures for the crystal structures are given in Table 3.6 (page 49) at the end of the chapter.

3.2 Crystal structure descriptions of the pure ligands

3.2.1 Crystal structure of **TER** as a tetrahydrate

Crystals suitable for SCD analysis were grown by slow evaporation of a solution of **TER** in a mixture of DMF and water. Two crystals, **TER-1** and **TER-2** were isolated. SCD analysis revealed that **TER-1** is a tetrahydrate form of **TER** while **TER-2** is a dihydrate form. The dihydrate form will be discussed in the next section. The tetrahydrate form crystallizes in the monoclinic space group $P2_1/c$. The asymmetric unit (Figure 3.1) consists of two water molecules and one **TER** molecule, with the latter located on an inversion centre.

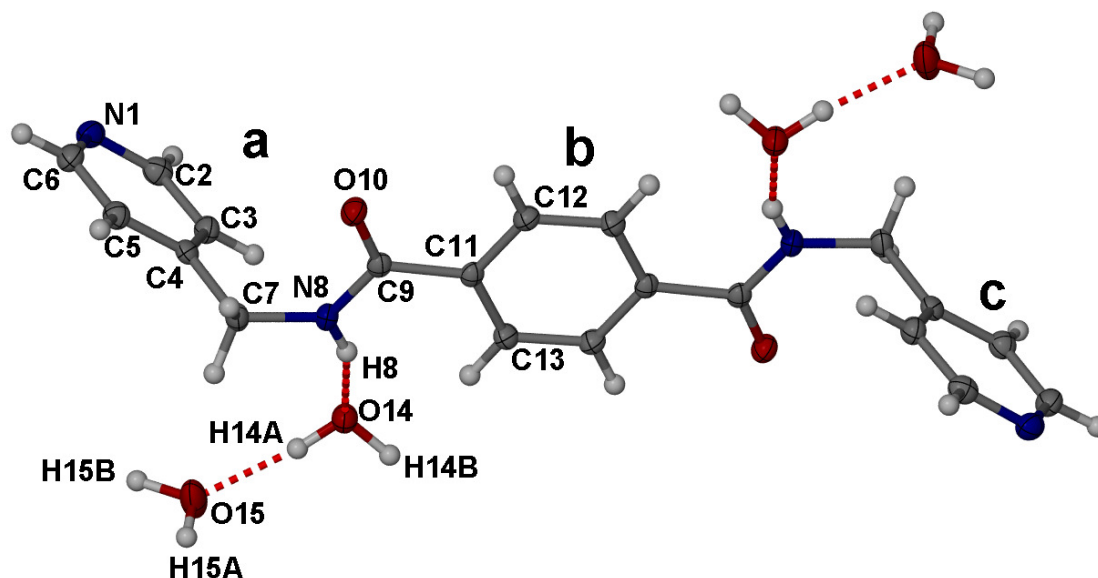


Figure 3.1. The molecular structure of **TER-1** showing the crystallographic labelling scheme for the asymmetric unit and 50% probability ellipsoids for non hydrogen atoms. Red dashed lines indicate hydrogen bonding. The three planes are labelled **a**, **b** and **c**.

The ligand adopts an **S** conformation with three planes labelled **a**, **b** and **c** as shown in Figure 3.1. Planes **a** and **c** represent the two 4-(aminomethyl)pyridine moieties while plane **b** represents the spacer group. The dihedral angle between the spacer group plane and the 4-(aminomethyl)pyridine plane is 79.88° (15). The amide groups are *trans* to each other, (torsion angles, 175.6° (2) and they are approximately co-planar with the phenylene ring.

Individual ligand molecules are aligned in a crisscross pattern in the *bc* plane, and they interact *via* the water molecules (Figure 3.2). One of the water molecules donates a hydrogen bond to the amide carbonyl group of a ligand ($O15 - H15B \cdots O10^{iii}$) as well as to the second water molecule ($O15 - H15A \cdots O14^{iv}$). The second water molecule, in turn, donates a hydrogen bond to a pyridyl nitrogen atom of a second ligand ($O14 - H14B \cdots N1^{ii}$) as well as to the other water molecule ($O14 - H14A \cdots O15$) (Figure 3.3). Finally, the second water molecule accepts a hydrogen bond from an amide NH group of third ligand molecule ($N8 - H8 \cdots O14^i$). A 3-D network is formed by virtue of these hydrogen bonds. All hydrogen bonding details are given in Table 3.1.

Table 3.1. Hydrogen-bond geometry (\AA , $^\circ$) for **TER-1**

$X-H \cdots A$	$X-H$	$H \cdots A$	$X \cdots A$	$\angle XHA$
$N8-H8 \cdots O14^i$	0.88	2.02	2.850(2)	155.7
$O14-H14B \cdots N1^{ii}$	0.97	1.83	2.766(2)	162.0
$O14-H14A \cdots O15$	0.89	1.84	2.728(2)	172.7
$O15-H15B \cdots O10^{iii}$	1.01	1.79	2.793(2)	179.6
$O15-H15A \cdots O14^{iv}$	0.85(2)	1.84	2.798(2)	178.2(2)

Symmetry codes: (i) $x, -y+3/2, z-1/2$, (ii) $-x, -y+2, -z+1$, (iii) $x-1, y, z$, (iv) $x-1, y, z$

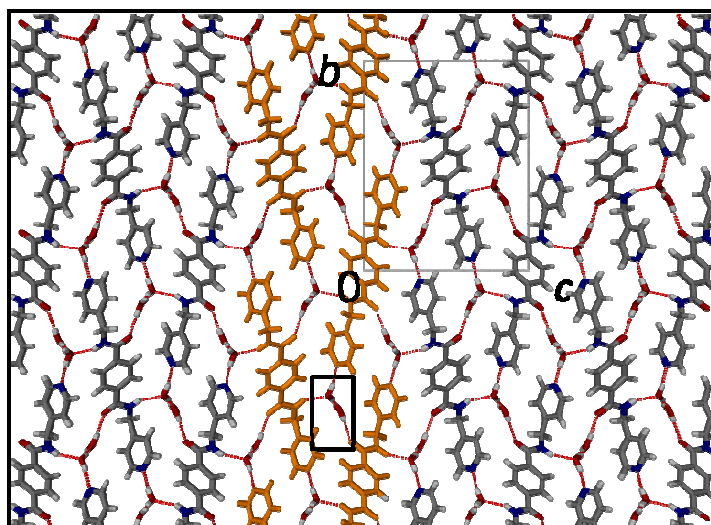


Figure 3.2. The packing diagram of **TER-1** as viewed down the *a* axis. The region within the inserted rectangle is shown magnified in Figure 3.3.

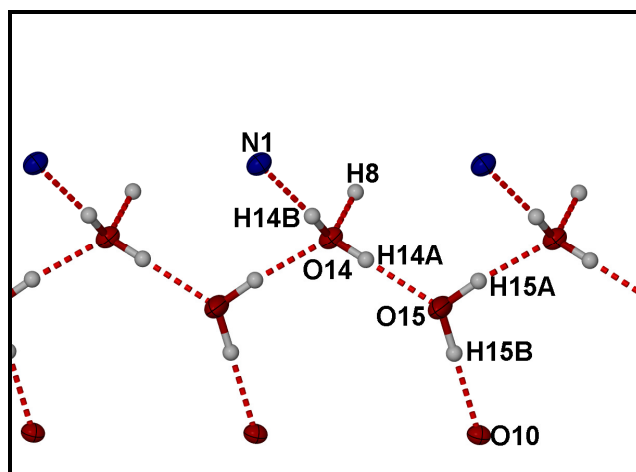


Figure 3.3. An expanded view of the hydrogen bonding interactions between individual **TER** and water molecules in **TER-1**.

3.2.2 Crystal structure of **TER** as a dihydrate

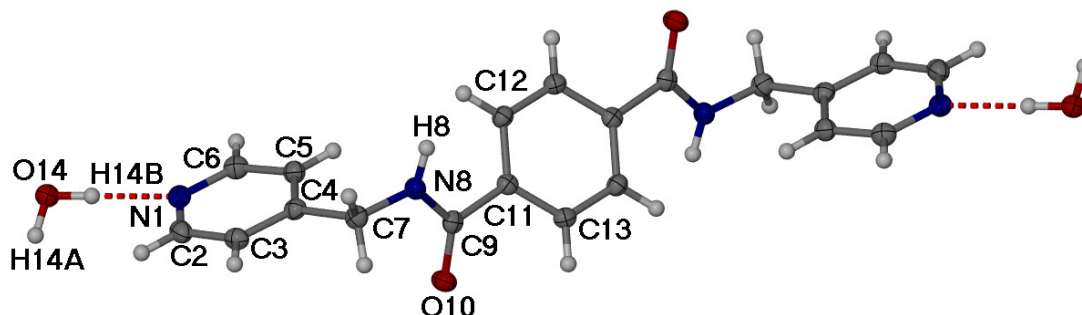


Figure 3.4. The molecular structure of **TER-2** showing the crystallographic labelling scheme and 50% probability ellipsoids for non-hydrogen atoms. Only the asymmetric unit is labelled.

The dihydrate form crystallizes in the orthorhombic space group *Pbca*. The asymmetric unit (Figure 3.4) consists of half a **TER** molecule, situated on an inversion centre and a water molecule. Unlike in the tetrahydrate structure, the amide groups are not co-planar with the phenylene ring, but are tilted at 32.95° (2) with respect to the phenylene ring plane. The 4-(aminomethyl)pyridine plane is almost perpendicular to the amide group plane (dihedral angle = 89.98° (3)).

Individual **TER** molecules interact by means of three hydrogen bonds *via* the water molecule. The water molecule is hydrogen bonded to the ligand *via* both the amide carbonyl group ($O14 - H14A \cdots O10^{ii}$) and the pyridyl nitrogen atom ($O14 - H14B \cdots N1$). In the third hydrogen bond, the water molecule acts as an acceptor of a hydrogen bond from the ligand *via* the amide NH group ($N8 - H8 \cdots O14^i$). In contrast to the tetrahydrate form of **TER**, hydrogen bonding between water molecules and **TER** results in a 2-D network (Figure 3.5). The 2-D

networks in the dihydrate form stack on top of one another as shown in Figure 3.6, with no significant π - π interactions observed. Details of hydrogen bonding are given in Table 3.2.

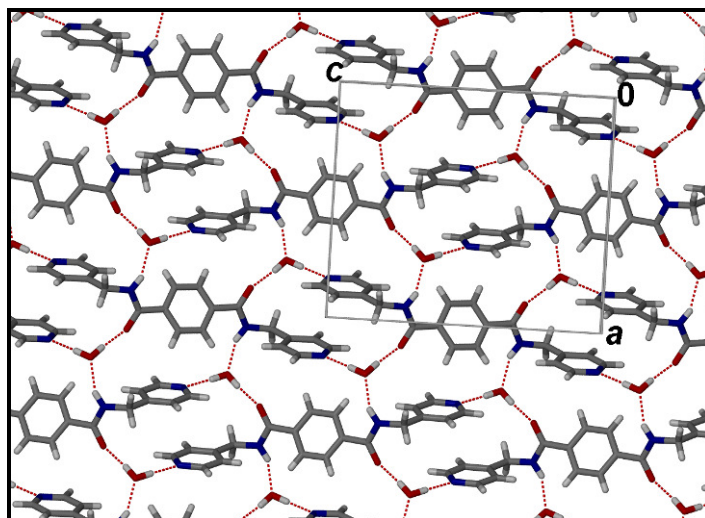


Figure 3.5. The packing diagram of **TER-2**. Individual **TER** molecules interact *via* the water molecule.

Table 3.2. Hydrogen-bond geometry (\AA , $^\circ$) for **TER-2**

$X-H\cdots A$	$X-H$	$H\cdots A$	$X\cdots A$	$\angle(XHA)$
$N8-H8\cdots O14^i$	0.88	2.02	2.838(3)	155.0
$O14-H14B\cdots N1$	0.93	1.93	2.846(3)	170.0
$O14-H14A\cdots O10^{ii}$	0.91	1.90	2.807(3)	174.6

Symmetry codes: (i) $-x-1/2, -y, z-1/2$, (ii) $-x, -y, -z+2$

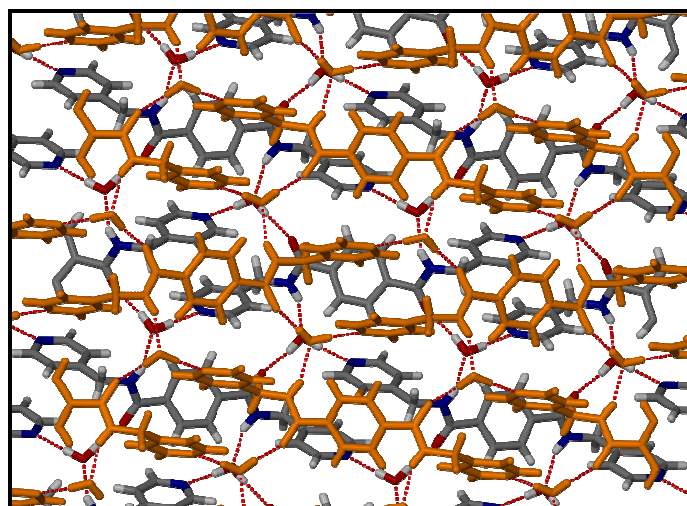


Figure 3.6. The 2-D networks formed as a result of the hydrogen bonding interactions between the water and **TER** molecules. The individual 2-D sheets are coloured in light brown and CPK colours to distinguish them from each other.

3.2.3 Crystal structure of ADI

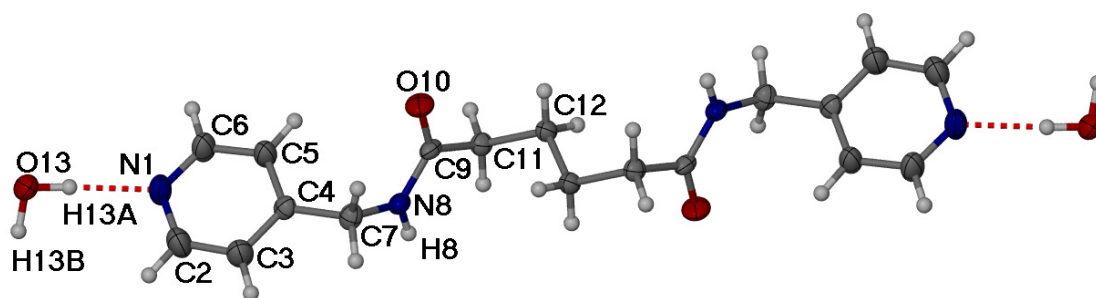


Figure 3.7. The molecular structure of **ADI** showing crystallographic labelling scheme and 30% probability ellipsoids for non-hydrogen atoms. Asymmetric unit atoms are labelled. Red dashed lines indicate hydrogen bonding.

Crystals suitable for SCD analysis were obtained from slow evaporation of an ethanolic solution of **ADI**. **ADI** crystallizes in the monoclinic space group $P2_1/c$. The asymmetric unit (Figure 3.7) consists of half an **ADI** molecule, situated on an inversion centre, and a water molecule.

The molecules are aligned to form two distinct columns with all molecules in one column sloping in one direction and molecules in the adjacent column sloping the other way to form a herringbone pattern. **ADI** molecules in the same column interact *via* self-complementary amide hydrogen bonds ($N8-H8 \cdots O10^i$).² The water molecule connects **ADI** molecules in adjacent columns by acting as a hydrogen bond donor in a hydrogen bond to the pyridyl nitrogen atom of a ligand in one column ($O13-H13A \cdots N1$) as well as in a hydrogen bond to the second water molecule ($O13-H13B \cdots O13^{ii}$), which in turn acts as a hydrogen bond donor to a pyridyl nitrogen atom of a ligand in the adjacent column ($O13-H13A \cdots N1$) (Figure 3.8). Details of all hydrogen bonding interactions are given in Table 3.3.

Table 3.3. Hydrogen-bond geometry (\AA , $^\circ$) for **ADI**

$X-H \cdots A$	$X-H$	$H \cdots A$	$X \cdots A$	$\angle(XHA)$
$N8-H8 \cdots O10^i$	0.88	1.94	2.814(2)	175
$O13-H13B \cdots O13^{ii}$	0.96	1.81	2.774(2)	173
$O13-H13A \cdots N1$	0.96	1.88	2.846(3)	173

Symmetry codes: (i) $x, y, z-1$, (ii) $x, -y+3/2, z-1/2$

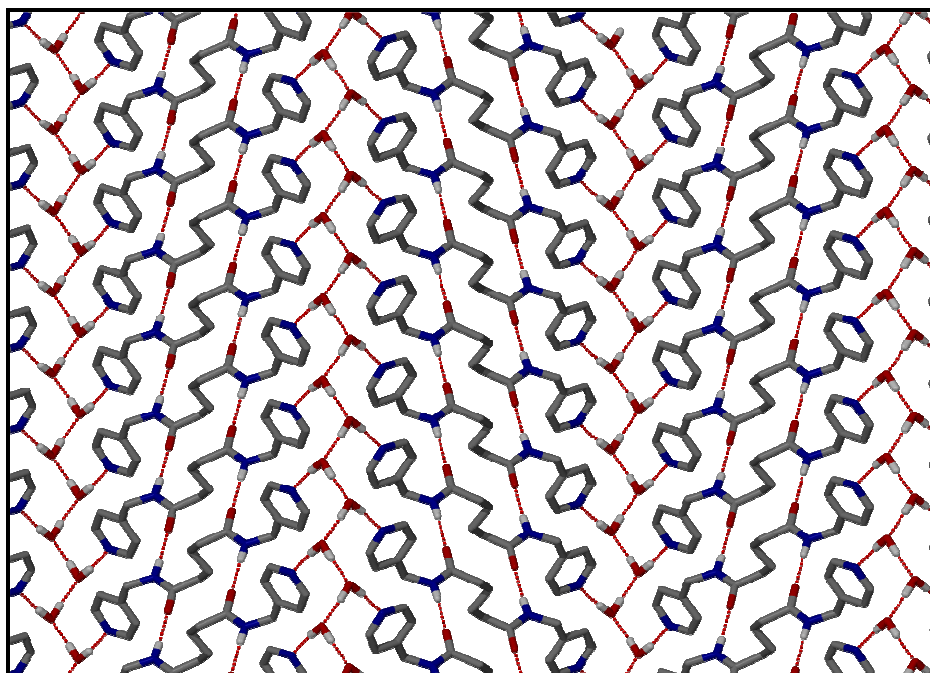


Figure 3.8. ADI molecules pack in the herringbone motif; molecules in the same column interact *via* self-complementary amide hydrogen bonds and molecules in adjacent columns are linked by hydrogen bonding *via* water molecules. Hydrogen atoms not involved in hydrogen bonding have been omitted for clarity.

3.2.4 Crystal structure of DIP

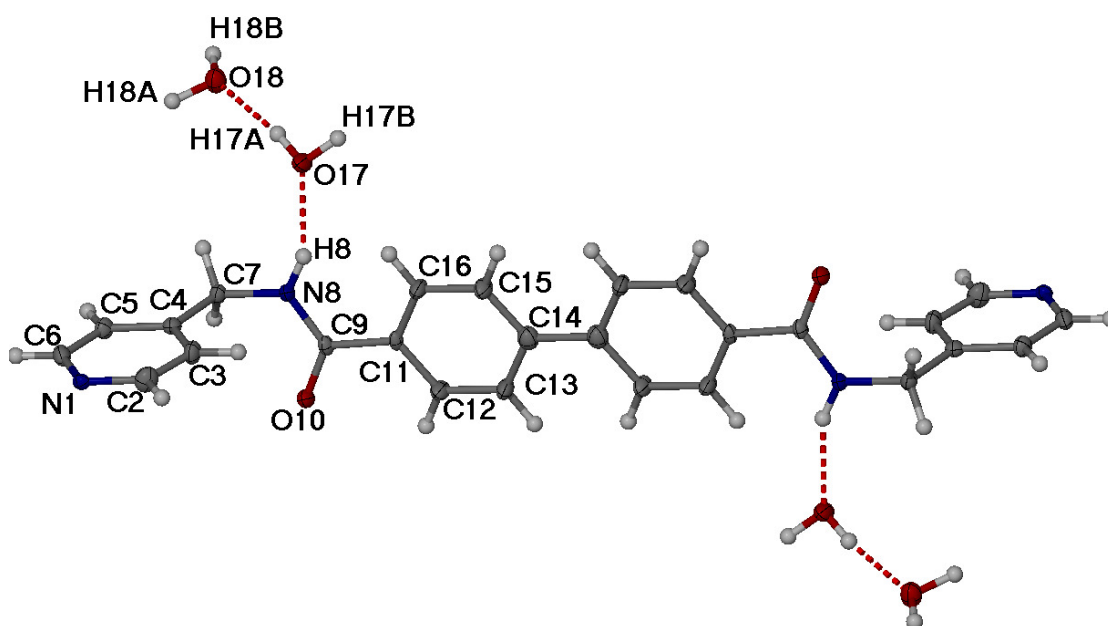


Figure 3.9. The molecular structure of **DIP** showing ellipsoids at 50% probability level and the crystallographic labelling scheme for the asymmetric unit. Red dashed lines indicate hydrogen bonding.

Crystals suitable for SCD analysis were obtained by slow evaporation of a solution of **DIP** in DMF. **DIP** crystallizes in the triclinic space group $P\bar{1}$. The asymmetric unit, which is shown in Figure 3.9, consists of half a **DIP** molecule which is situated on an inversion centre as well as

two water molecules. The ligand adopts an elongated *S* conformation with the two amide groups *trans* to each other with respect to the biphenyl moiety. The amide group is tilted 12.68° (16) and 81.89° (18) relative to the planes of the biphenyl and the 4-(aminomethyl)pyridine groups, respectively.

Ligand molecules interact *via* the water molecules. The ligand is hydrogen bonded *via* the amide group ($N8-H8 \cdots O17$) to a water molecule, which is in turn hydrogen bonded *via* the amide carbonyl group ($O17-H17B \cdots O10^{ii}$) to a second ligand molecule as well as to the second water molecule ($O17-H17A \cdots O18$). The second water molecule is in turn hydrogen bonded to a second ligand molecule *via* amide carbonyl group ($O18-H18B \cdots O10^{ii}$) and to a third ligand molecule *via* the pyridyl nitrogen atom ($O18-H18A \cdots N1^i$). By virtue of these hydrogen bonding interactions, the pyridine moieties are stacked on top of one another to form a motif that resembles a staircase. The packing diagram and the hydrogen bonding can be seen in Figures 3.10 and 3.11 respectively. Hydrogen bonding details are given in Table 3.4.

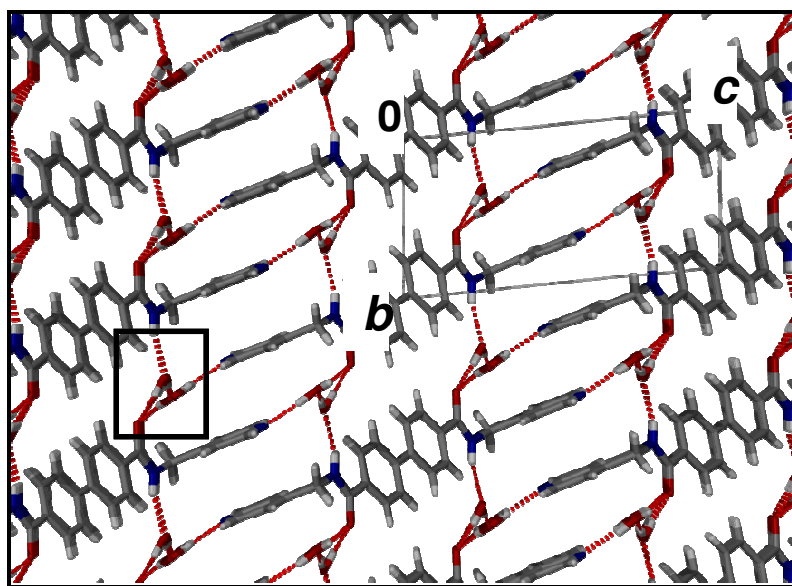


Figure 3.10. The packing diagram of **DIP** as viewed along the *a* axis. The region within the inserted rectangle is shown magnified in Figure 3.11.

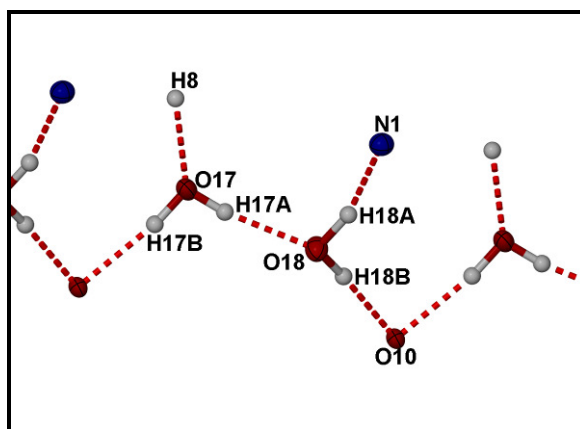


Figure 3.11. The expanded view of the hydrogen bonding interaction between **DIP** and water molecules.

Table 3.4. Hydrogen-bond geometry (\AA , $^\circ$) for **DIP**

X—H \cdots A	X—H	H \cdots A	X \cdots A	$\angle(\text{XHA})$
N8—H8 \cdots O17	0.88	1.99	2.822(2)	156.2
O18—H18A \cdots N1 ⁱ	0.98	1.829	2.776(2)	155.5
O17—H17A \cdots O18	0.85	1.91	2.757(2)	170.7
O18—H18B \cdots O10 ⁱⁱ	0.97	1.88	2.843(2)	172.6
O17—H17B \cdots O10 ⁱⁱⁱ	0.91	1.91	2.810(2)	171.8

Symmetry codes: (i) $-x+1, -y, -z+1$, (ii) $x+1, y-1, z$, (iii) $x, y-1, z$

3.2.5 Crystal structure of GLUT

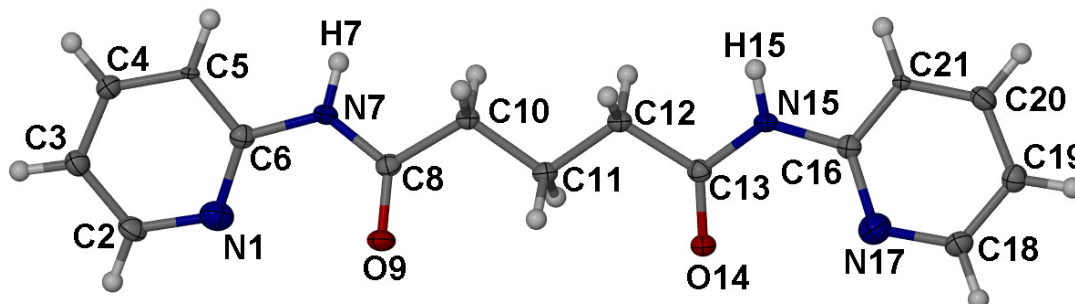


Figure 3.12. The asymmetric unit of **GLUT** showing the crystallographic labelling scheme and displacement ellipsoids at 50% probability level.

Crystals suitable for SCD analysis were grown by slow evaporation of an ethanolic solution of **GLUT**. The ligand crystallizes in the monoclinic space group $P2_1/c$ with an entire **GLUT** molecule in the asymmetric unit (Figure 3.12). The two pyridyl nitrogen atoms face the same side as the two oxygen atoms of the amide group. A trend that has been observed so far is that water molecules and/self-complementary amide hydrogen bonds connect individual ligand molecules. However, in the crystal structure of **GLUT**, neither self-complementary amide hydrogen bonds nor water molecules occur. Individual ligand molecules interact *via* amide NH and aromatic CH groups to form crisscross 1-D chains running along $[001]$ (Figure 3.13a).

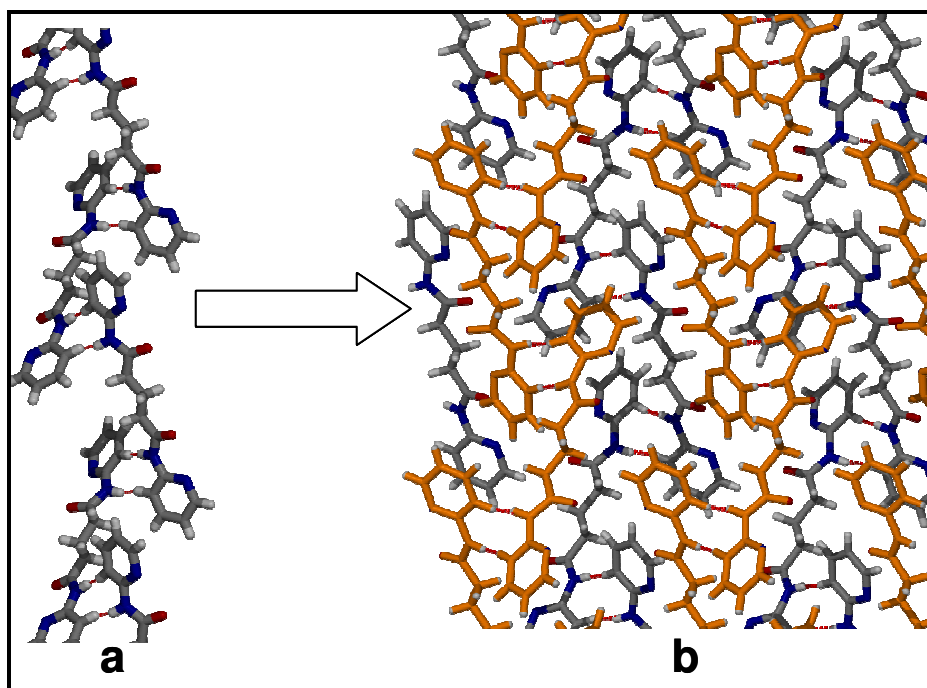


Figure 3.13. (a) Crisscross 1-D chains formed as a result of hydrogen bond interaction between amide NH and aromatic CH groups of neighbouring **GLUT** molecules, (b) packing diagram showing chains in the two layers coloured in light brown and CPK colours.

The 1-D chains pack to form layers; chains in the same layer do not interact by any type of hydrogen bond. However, they do interact with chains in the next layer *via* π - π interactions as evidenced by a centroid-to-centroid distance of 3.691 Å (Figure 3.13b).

3.2.6 Crystal structure of **TER-A**

Crystals suitable for SCD analysis were obtained by slow evaporation of a DMF solution of **TER-A**. The asymmetric unit of **TER-A** (Figure 3.14) consists of one entire **TER-A** molecule. The ligand comprises two distinct planes: one formed by the 4-(aminomethyl)pyridine moiety and the other formed by the benzoic acid moiety. The dihedral angle between the two planes is 79.76°. The carboxylic acid and pyridyl groups are well-known for combining to generate α -networks,³ while amide bonds are well-known for forming self-complementary amide hydrogen bonds.² In the crystal structure of **TER-A** both interactions are observed. Individual ligand molecules interact *via* the pyridine-carboxylic acid interaction to form an α -network (O19 – H19 \cdots N1ⁱⁱ). Ligand molecules in the parallel 1-D chains interact *via* self-complementary amide hydrogen bonds (N8 – H8 \cdots O10ⁱ) to form a β -network. The β -sheets stack directly on top of one another (Figure 3.15). Hydrogen bonding details are given in Table 3.5.

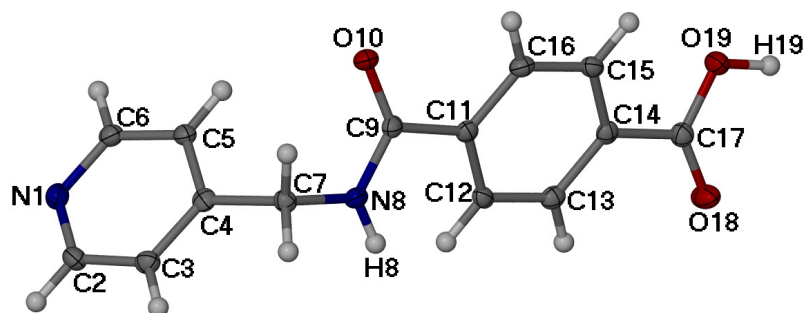


Figure 3.14. The asymmetric unit of **TER-A** showing the crystallographic labelling scheme and 50% probability ellipsoids for non-hydrogen atoms.

Table 3.5. Hydrogen-bond geometry (\AA , $^\circ$) for **TER-A**

$X-H\cdots A$	$X-H$	$H\cdots A$	$X\cdots A$	$\angle(XHA)$
$N8-H8\cdots O10^i$	0.88	2.12	2.875(2)	144.1
$O19-H19\cdots N1^{ii}$	1.04	1.54	2.573(1)	177.3

Symmetry codes: (i) $-x+3/2, y, z+1/2$, (ii) $x+1/2, -y, z$

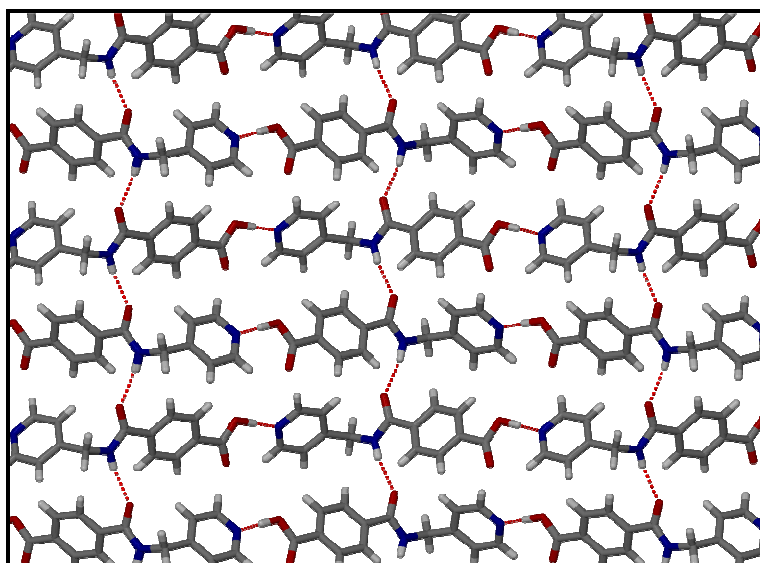


Figure 3.15. The packing diagram of **TER-A**. Individual **TER-A** molecules interact *via* complementary amide to amide hydrogen bonds as well as PY-N \cdots H-O hydrogen bonds.

3.3 Conclusion

The crystal structures of **TER**, **ADI**, **DIP**, **GLUT** and **TER-A** are described here. Even though crystallizations were carried out in either ethanol/DMF, none of the crystal structures included any of these solvent molecules. All the crystal structures, except **GLUT** and **TER-A**, included water molecules which play the role of linking ligand molecules *via* hydrogen bonding. In the crystal structure of **GLUT**, the ligand molecules interact *via* hydrogen bonding between the amide NH and the aromatic CH groups as well as π - π interactions between the pyridyl rings to

form an assembly with no space for water molecules. Of the six structures, only the crystal structures of **ADI** and **TER-A** featured the self-complementary amide hydrogen bonds. It is not clear why these interactions are absent in the rest of the crystal structures. Perhaps the interactions between the amide groups and water molecules are more favourable than the interactions between amide groups.

3.4 References

1. G. O. Lloyd, *Acta Cryst. Sect. E*, 2005, **E61**, o1218.
2. R. Taylor and O. Kennard, *Acc. Chem. Res*, 1984, **17**, 320.
3. E. Matwey, C. L. Schauer, F. W. Fowler, and J. W. Lauher, *J. Am. Chem. Soc*, 1997, **119**, 10245.

Table 3.6. Crystallographic data of the synthesized ligands

	TER-1	TER-2	ADI	DIP	GLUT	TER-A
Empirical formula	C ₂₀ H ₂₆ N ₄ O ₆	C ₂₀ H ₂₂ N ₄ O ₄	C ₁₈ H ₂₆ N ₄ O ₄	C ₂₆ H ₃₀ N ₄ O ₆	C ₁₅ H ₁₆ N ₄ O ₂	C ₂₈ H ₂₄ N ₄ O ₆
Formula weight	418.45	382.42	362.43	494.54	284.32	512.51
Temperature (K)	173(2)	173(2)	173(2)	173(2)	173(2)	173(2)
Wavelength (Å)	0.71073	0.71073	0.71073	0.71073	0.71073	0.71073
Crystal system	monoclinic	orthorhombic	monoclinic	triclinic	monoclinic	orthorhombic
Space group	<i>P2₁/c</i>	<i>Pbca</i>	<i>P2₁/c</i>	<i>P$\bar{1}$</i>	<i>P2₁/c</i>	<i>Pca2₁</i>
<i>a</i> /Å	4.7486(7)	12.843(2)	7.6077(2)	6.496(2)	8.188(1)	26.365(5)
<i>b</i> /Å	16.728(2)	9.608(1)	27.665(6)	6.928(2)	15.767(3)	4.524(9)
<i>c</i> /Å	13.396(2)	14.965(2)	4.849(1)	13.656(4)	10.9328(2)	9.786(2)
α /°				84.061(4)		
β /°	100.073(2)		105.76(3)	88.035(4)	102.078(2)	
γ /°				79.946(4)		
Volume (Å ³)	1047.7(3)	1847(4)	982.4(3)	602.1(3)	1380.2(4)	1167.3(2)
<i>Z</i>	2	4	2	1	4	2
Calculated density (g cm ⁻³)	1.326	1.376	1.225	1.364	1.368	1.458
Absorption coefficient (mm ⁻¹)	0.099	0.098	0.088	0.098	0.094	0.105
<i>F</i> ₀₀₀	444	808	388	262	600	536
Crystal size (mm ³)	0.37 × 0.26 × 0.11	0.29 × 0.16 × 0.05	0.30 × 0.22 × 0.19	0.20 × 0.16 × 0.12	0.38 × 0.33 × 0.23	0.24 × 0.18 0.16
θ range for data collection (°)	1.97 to 28.14	2.72 to 27.99	2.78 to 27.10	1.50 to 28.18	2.30 to 27.94	1.54 to 25.60
Miller index ranges	-5 ≤ <i>h</i> ≤ 6, -21 ≤ <i>k</i> ≤ 21, -17 ≤ <i>l</i> ≤ 17	-16 ≤ <i>h</i> ≤ 16, -12 ≤ <i>k</i> ≤ 12, -19 ≤ <i>l</i> ≤ 18	-9 ≤ <i>h</i> ≤ 6, -34 ≤ <i>k</i> ≤ 35, -5 ≤ <i>l</i> ≤ 6	-8 ≤ <i>h</i> ≤ 8, -9 ≤ <i>k</i> ≤ 9, -18 ≤ <i>l</i> ≤ 17	-9 ≤ <i>h</i> ≤ 10, -20 ≤ <i>k</i> ≤ 18, -14 ≤ <i>l</i> ≤ 13	31 ≤ <i>h</i> ≤ 32, -5 ≤ <i>k</i> ≤ 4, -11 ≤ <i>l</i> ≤ 6
Reflections collected	11628	19267	5441	6780	8226	5909
Independent reflections	2439 [<i>R</i> _{int} = 0.0364]	2148 [<i>R</i> _{int} = 0.0778]	2123 [<i>R</i> _{int} = 0.0293]	2628 [<i>R</i> _{int} = 0.0256]	3010 [<i>R</i> _{int} = 0.0280]	1615 [<i>R</i> _{int} = 0.0280]
Completeness to θ_{\max} (%)	94.8	96.6	98.1	88.7	90.7	99.8
Max. and min. transmission	0.9892 and 0.9642	0.9951 and 0.9722	0.9835 and 0.9741	0.9883 and 0.9806	0.9786 and 0.9650	0.9835 and 0.9753
Refinement method	Full-matrix least-squares on <i>F</i> ²	Full-matrix least-squares on <i>F</i> ²	Full-matrix least-squares on <i>F</i> ²	Full-matrix least-squares on <i>F</i> ²	Full-matrix least-squares on <i>F</i> ²	Full-matrix least-squares on <i>F</i> ²
Data / restraints / parameters	2439 / 0 / 143	2148 / 0 / 129	2123 / 2 / 126	2628 / 0 / 170	3010 / 0 / 190	1615 / 1 / 173
Goodness-of-fit on <i>F</i> ²	1.037	1.016	1.033	1.047	1.002	1.059
Final <i>R</i> indices [<i>I</i> > 2 σ (<i>I</i>)]	<i>R</i> 1 = 0.0385, <i>wR</i> 2 = 0.0863	<i>R</i> 1 = 0.0452, <i>wR</i> 2 = 0.0974	<i>R</i> 1 = 0.0613, <i>wR</i> 2 = 0.1383	<i>R</i> 1 = 0.0436, <i>wR</i> 2 = 0.1077	<i>R</i> 1 = 0.0763, <i>wR</i> 2 = 0.2221	<i>R</i> 1 = 0.0273, <i>wR</i> 2 = 0.0676
<i>R</i> indices (all data)	<i>R</i> 1 = 0.0549, <i>wR</i> 2 = 0.0959	<i>R</i> 1 = 0.0806, <i>wR</i> 2 = 0.1143	<i>R</i> 1 = 0.0994, <i>wR</i> 2 = 0.1570	<i>R</i> 1 = 0.0606, <i>wR</i> 2 = 0.1185	<i>R</i> 1 = 0.0927, <i>wR</i> 2 = 0.2384	<i>R</i> 1 = 0.0302, <i>wR</i> 2 = 0.0700
Largest diff. peak and hole (e Å ⁻³)	0.331 and -0.230	0.216 and -0.221	0.149 and -0.172	0.375 and -0.258	0.825 and -0.852	0.153 and -0.173